Geological Setting of Gold Bearing Quartz Veins in the Aureole of the Sabaskong Batholith at Nestor Falls, Ontario

Honours BSc 4490 Senior Thesis

Department of Earth Sciences

The University *of* Western Ontario

Roderick Tom-Ying

Supervised by Dr. Norman A. Duke

April 2012

Abstract

The Wagg and Galbraith gold prospects, owned by Kings Bay Gold Corp, is located in the western Wabigoon Subprovince, 16 km south of Nestor Falls, Ontario. Bulk rock geochemical results demonstrate the gold-bearing quartz veins are hosted by iron rich tholeiitic pillow basalt within the thermal aureole of the Sabaskong Batholith. Mineral chemistry demonstrates that the pillow basalts have undergone prograde metamorphism to hornblende stable thermal conditions. Extensive felsic porphyritic dykes inject the amphibolitic basalt at peak metamorphic conditions. Geochemical analyses of dykes show total SiO_2 contents range from 61-69% and high Na/K ratios, indicative of dacitic melt compositions. Calc-silicate flooding is attributed to CO_2 devolatilization within the aureole. A series of brittle to ductile shears formed in proximity to zones of felsic dyking. Limited biotitization of shear domains occurred due to retrograde reactions under mid-greenschist facies conditions. This study supports hydrothermal concentration of free gold in quartz veins occurring at porphyry dyke margins during retrograde cooling.

Table of Contents

Acknowledgements

I would like to thank Russell Crosby, P.Geo, Kyle Picard, Ray Préfontaine, and the rest of the Kings Bay Gold crew for supporting me in this endeavor. Kings Bay Gold has generously funded this project including airfares, meals, and accommodations. Special acknowledgement must be given to President Kyle Picard for arranging for Accurassay's sponsorship of geochemistry analysis.

Thank you Steve Wood for the prompt creation of polished thin sections. Thanks Jim Renaud for your precise and accurate electron micro-probe results.

A special thanks to Dr. Norman Duke for taking on the monumental task of supervising, particularly for timely editing of drafts, this would not be possible without your guidance. Lastly, I would like to acknowledge my friends and family for their undying support.

Chapter 1 – Introduction

1.1 Opening Statement

Kings Bay Gold, based out of Winnipeg, Manitoba, currently has two active projects in Menary Township, south of Nestor Falls; the Wagg and Galbraith drill sites. Nestor Falls, located 2 hours south of Kenora, Ontario, lies within the geological region known as the Wabigoon Subprovince of the Canadian Shield. On October 27-30th, 2011 a site visit was undertaken with Dr. Norman Duke, Carl Archibald and P.Geo Russell Crosby to view outcrops and sample drill core for detailed petrographic and geochemical analyses.

1.2 Geographic Location & Physiography

Located on the western portion of the Wabigoon Subprovince, Nestor Falls is accessible by the Trans Canada Highway 17 and 71. It is located 4.5 hours southeast from Winnipeg or 6 hours from Thunder Bay (Figure 1). The location of the Wagg and Galbraith projects are 16 km south of Nestor falls on highway 71, followed by 4km on an old graveled logging road (road 404), with the last 2 km accessible only by off-road vehicles.

Menary Township is home to a boreal forest of black and white spruce, jack pine, poplars and white birch. There is approximately 15-25% outcrop exposure. Highly

conductive glaciolacustrine silts and clays of the Glacial Lake Agassiz cover the bedrock. Till and vegetation stripping completed in 2010 cleared the Wagg drill site and in 2011 cleared the Galbraith site, allowing 85+% outcrop exposure. The topography at both the Wagg and Galbraith prospects has relatively high relief as they are situated within the aureole of the Sabaskong batholith.

Figure : Regional Map Depicting Location of Nestor Falls and Surrounding Area

1.3 Background

A report written by Western Troy Capital Resources in January 1993 describes the regional geology of Menary Township. The basement lithologies of the Wabigoon Subprovince are extensively covered and includes mafic to intermediate metavolcanic rocks such as pillow basalt flows, gabbro sills, andesite flows, and tuffs. The grade of metamorphism of the Archean volcanics range from regional greenschist facies to amphibolite facies at the margin of granitic intrusions. Medium grained porphyritic rhyolites and dacites as well as ubiquitous feldspar porphyry dykes are observed. Archean intermediate to felsic intrusive rocks intrude the metavolcanics. Precambrian diabase dykes postdate the felsic intrusions. Bedrock is overlain by till, sand, gravel, and clay from the Quaternary glaciation. The quartz veins carrying traces of gold occur in the domains of felsic dykes.

In a paper entitled “Background and Anomalous Gold in Rocks of an Archean Greenstone Assemblage, Kakagi Lake Area, Northwestern Ontario, Kwong and Crocket (1978) seek to identify lithologies that act as preferred hosts for gold deposition. These authors analyzed various rock lithologies for background gold by neutron activation methods. The lithologies included mafic volcanics, metasedimentary rocks, felsic volcanics, mafic-ultramafic intrusions and felsic plutonic stocks. Their results demonstrated background levels of 1-2 ppb gold within the Archean greenstones. Gold levels of 10 ppb or greater occurs in “quartz veins, carbonate zones, shear zones, and

felsic dykes" leading the researchers to believe that gold deposition in the Wabigoon Subprovince is associated with felsic dyking.

A paper seeking to explain the heat flow in the western Superior Province may hint at the timing required for a large-scale heat flow event that drives gold deposition. Entitled "Heat Flow in the western Superior Province of the Canadian shield", Rolandone et. al. (2003) demonstrate that on a regional scale there was no significant variation of crustal heat production much past 2.7 Ga. This infers that post cratonization, the crust lacked heat needed to drive hydrothermal alteration or fluid flow for gold deposition. By drawing upon conclusions from Kwong and Crocket (1978), it is theorized that any gold deposition that occurs in the Wabigoon Subprovince is related to terminal Archean orogeny.

In a paper entitled: "A review of the Superior Province of the Canadian Shield, product of Archean accretion" Card (1990) examines the formation of the Superior Province. By using uranium-lead isotopic dating, Card, was able to constrain the age of the Superior Province between 3.1 Ga aged high-grade gneiss to 2.68 Ga for calc-alkaline plutonism. The paper also provides an examination of the late orogenic Timiskaming-type shoshonitic/alkalic volcanic-fluvial sediments.

Hall & Millar (1987) provide an in depth analysis of the local Sabaskong batholith occurring within Menary Township, is based on gravity and aeromagnetic surveys. In Menary Township, the Sabaskong batholith strikes at N65E. Hall & Millar describes the Sabaskong batholith as a multiphase body consisting of granodiorite, quartz monzonite and trondhjemite. Radial magnetic anomaly trends over the batholith may be a reflection of deep crustal magnetization.

1.4 Purpose of Study

Although extensive work has been conducted on the Wabigoon Subprovince at the Rainy River mining camp, little research has yet addressed Menary Township area near Nestor Falls. The primary focus of the present study is to document the prograde/retrograde overprint of the host pillow lavas through detailed petrographic and microprobe analysis of polished thin-sections. Early calc-silication at amphibolite facies conditions is followed by the biotitization of ductile shear zones. These alterations may be linked to pegmatite genesis. Bulk rock geochemistry results, based on samples collected at the Wagg and Galbraith prospects, demonstrate the effects of calc-silicate and biotite alteration on their host amphibolitic pillow basalts.

Chapter 2 – Regional Geology

2.1 General Statement

The Wagg and Galbraith prospects occur in the western portion of the Wabigoon Subprovince. The Sabaskong batholith, covering up to 2500 km^2 underlies a large central area (Hall and Millar, 1987). Metamorphism of marginal volcanics reaches amphibolite facies. The following outline of the regional geology is derived from Kwong (1978), Hall and Millar (1987), Blackburn (1988), Card (1990), Barron (1996), and Percival et. al (2006).

2.2 The Western Wabigoon Subprovince

The Superior Province is known as the world's largest Archean craton (Percival et. al, 2006). It consists of high-grade gneiss in the northern and southern subprovinces while alternating belts of granite-greenstone and metasediments make up the central regions. The granite-greenstone belts are typified by mafic meta-volcanics, representing arc volcanism. Old platform sequences consisting of quartz arenite-stromatolitic carbonate and late orogenic sequences of Timiskaming-type shoshonitic/alkalic volcanic-fluvial sediments occur locally within the greenstone belts. Timiskaming-type sequences are deposited in pull-apart basins developed along strike-slip faults during the late Archean (Card, 1990).

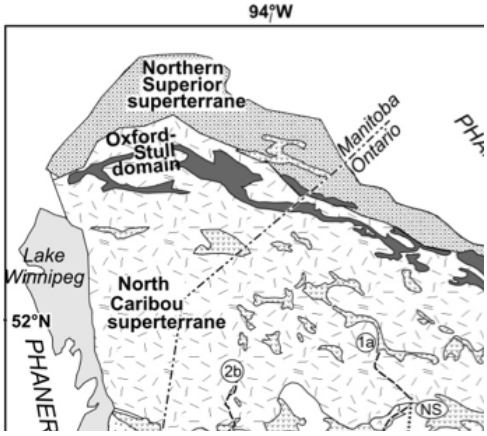

The Wabigoon volcanic-plutonic Subprovince occupies the western portion of the Superior Province (Figure 2 &3). The Wabigoon consists of tholeitic and calc-alkaline volcanics dated between 3.2-2.71 Ga, that have been intruded by granitoid plutons dated between 2710-2695 Ma (Blackburn et al., 1988), (Card, 1990). Sixty five percent of the rocks are plutonic, the remaining 35% as supracrustal. Of the supracrustal lithologies, 60% are tholeiitic volcanics, 30% calc-alkaline volcanics and 10% are metasedimentary.

The supracrustal rocks of the eastern Wabigoon greenstone belt consist of similar lithologies and age as the western Subprovince with the main difference being the appearance of a 3.0 Ga supracrustal sequence of quartzite, iron formations and argillite at Atikokan.

Supracrustal rocks of the Western Wabigoon region consists of a lower mafic sequences (known as the Keewatin Series) overlain by intermediate to felsic metavolcanics. The lower mafic Keewatin Series is dated at 2,775 Ma. Mg-rich pillow to massive tholeiitic basalt flows are continuous. Upper mafic sequences of komatiitic and tholeiitic mafic flows date between 2,729-2,725 Ma. Medium grained quartz-feldspar porphyries inject the pillow basalts. Timiskaming-type alluvial/fluvial conglomerate, sandstone, siltstone and thick turbiditic sequence overlie the western Wabigoon metavolcanics (Card, 1990). The Timiskaming-type conglomerate-sandstone sequences occur within the Seine River fault, forming the subprovincial boundary between the Wabigoon Subprovince and the southern Quetico Subprovince (Card, 1990).

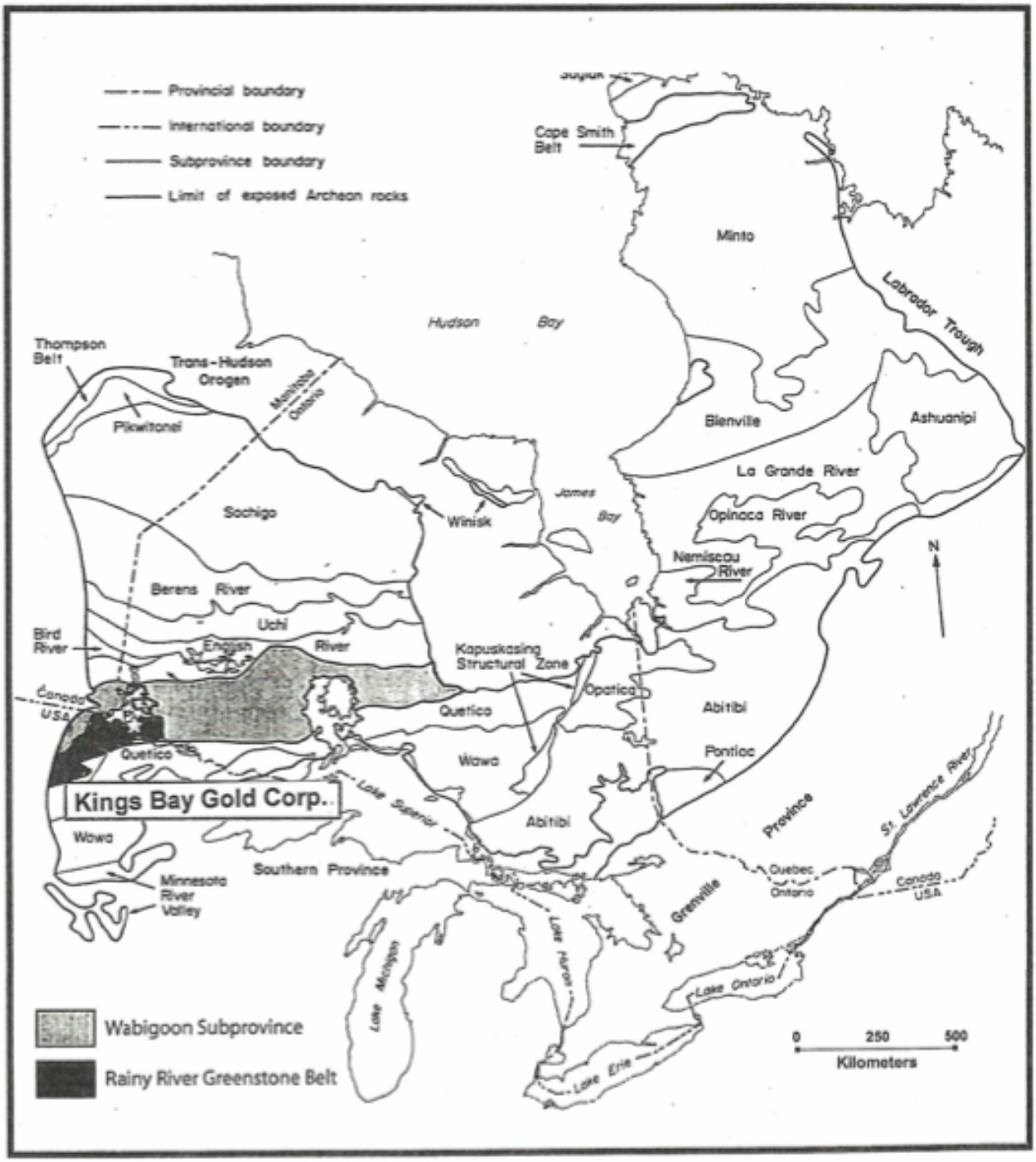

Figure 3: Regional Geological Setting of the Wabigoon Subprovince and King's Bay Gold Prospects

Chapter 3 – Local Geology

3.1 General statement

King's Bay Gold, based out of Winnipeg, Manitoba, currently owns 10 unpatented claims in Menary Township, expanding an original core group of 4 purchased in January 2010 (Figure 4). The Menary prospect is centered on auriferous veins hosted within amphibolite facies mafic volcanics bordering the Sabaskong batholith.

3.2 Menary Township

King's Bay Gold's prospects are situated in amphibolitic pillow basalts on the margin of the Sabaskong Batholith (Figures 4 and 5). The grade of metamorphism within the volcanic rocks increases from lower greenschist facies to amphibolite facies at the batholith contact. The metavolcanic rocks trend northeasterly parallel to the batholith (Figure 6). King's Bay Gold drilling program intersected marginal granodiorite at the Galbraith prospect.

The margin of the Sabaskong batholith consists of granitic agmatitic breccia with amphibolitic rafts intruded by pink felsic dykes. The interior of the batholith exposed at Nestor Falls is characterized by moderately dipping orthogneiss with transposed mafic rafts. Holmstead (1993) describes the dykes injecting the batholith contact as narrow, granitic textured, offshoots into mafic meta-volcanic country rock. The gold mineralization in the thermal aureole of the Sabaskong batholith occurs proximal to dyking (Figure 4).

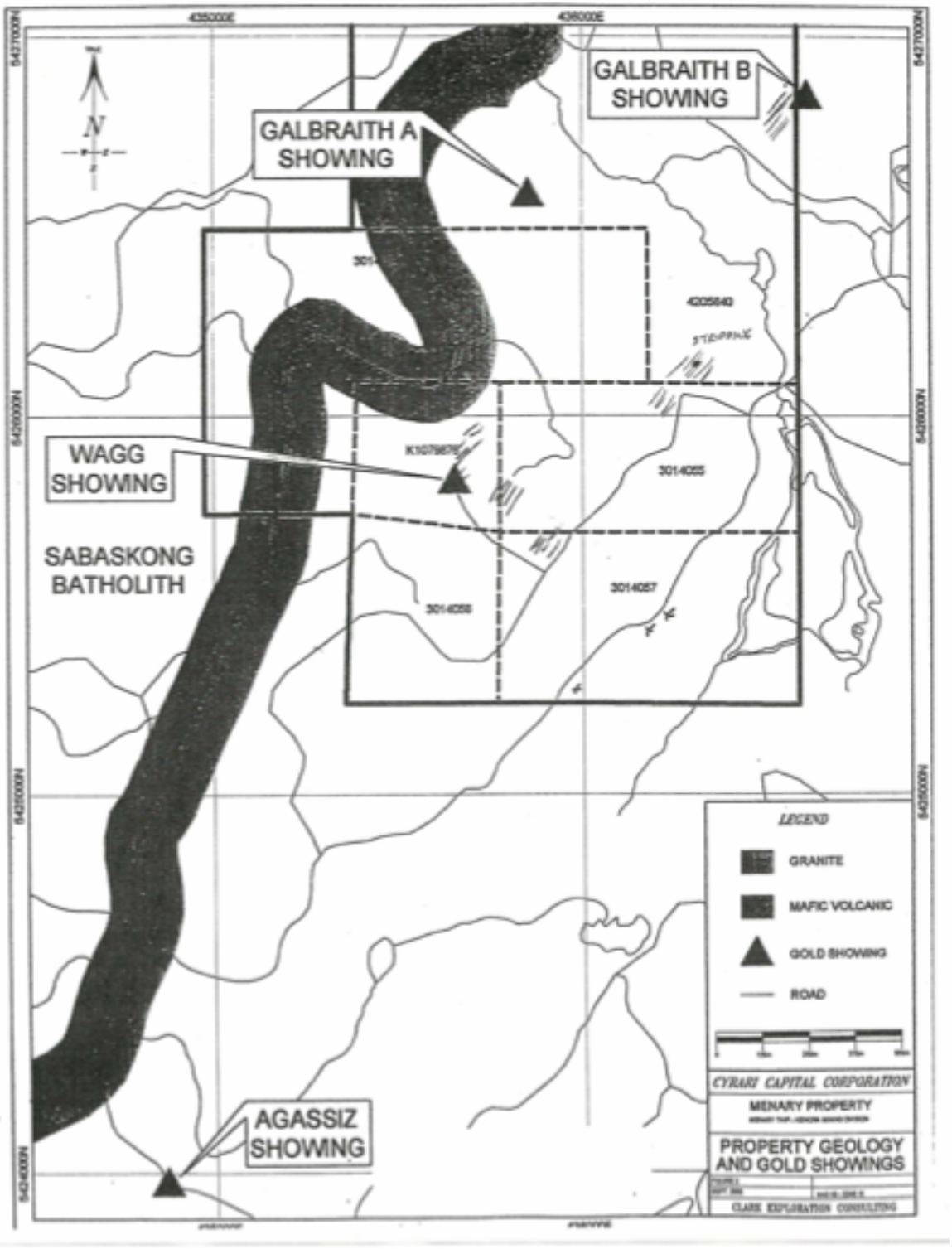
435000E
436000E
5427000N
5426000N
5425000N
5424000N
N
GALBRAITH A SHOWING
GALBRAITH B SHOWING
WAGG SHOWING
AGASSIZ SHOWING
SABASKONG BATHOLITH
4205640
3014055
3014057
3014058
LEGEND
GRANITE
MAFIC VOLCANIC
GOLD SHOWING
ROAD
CYRARI CAPITAL CORPORATION
MENARY PROPERTY
PROPERTY GEOLOGY AND GOLD SHOWINGS
CLARE EXPLORATION CONSULTING

3.3 Wagg Prospect

The Wagg prospect consists of 6 en-echelon quartz veins sited proximal to pinkish-brown weathered feldspar porphyry dykes, these are well exposed in trenches 1-4 (Figure 5). The extent of the diamond drilling is shown in Figure 5 with the drill holes oriented at 45 degrees to SE. Variably preserved pillow lavas host the intermediate to felsic porphyry dikes. Late tectonic K-metasomatism focused within shears drive retrograde reactions after peak amphibolite metamorphic conditions. The dikes have been sheared and these shears host the crack-seal style gold-bearing quartz veins. Veinlets of white sugary quartz, ranging from 0.5cm-1m wide, are ubiquitous in shear domains. The auriferous vein selvages exhibit moderate biotitization that overprints the amphibolite facies textures. The quartz veins exposed in trenches 1-4 are typically orangish-red in colour due to hematite alteration. These veins carry pyrite and weather into a dark cherry red colour, indicating strong hematization of pyrite. Gold deposition is favoured in the orangish-red quartz veins indicating association with pyrite. However, recrystallized sugary white quartz can also contain free coarse grains of gold with negligible associated sulphide. Bulk sampling at Wagg shows the highest gold content is associated with orangish-red quartz veins containing visible disseminated pyrite rather than sugary white recrystallized quartz veins.

Figure 5: Drill Hole Placement at the Wagg Prospect

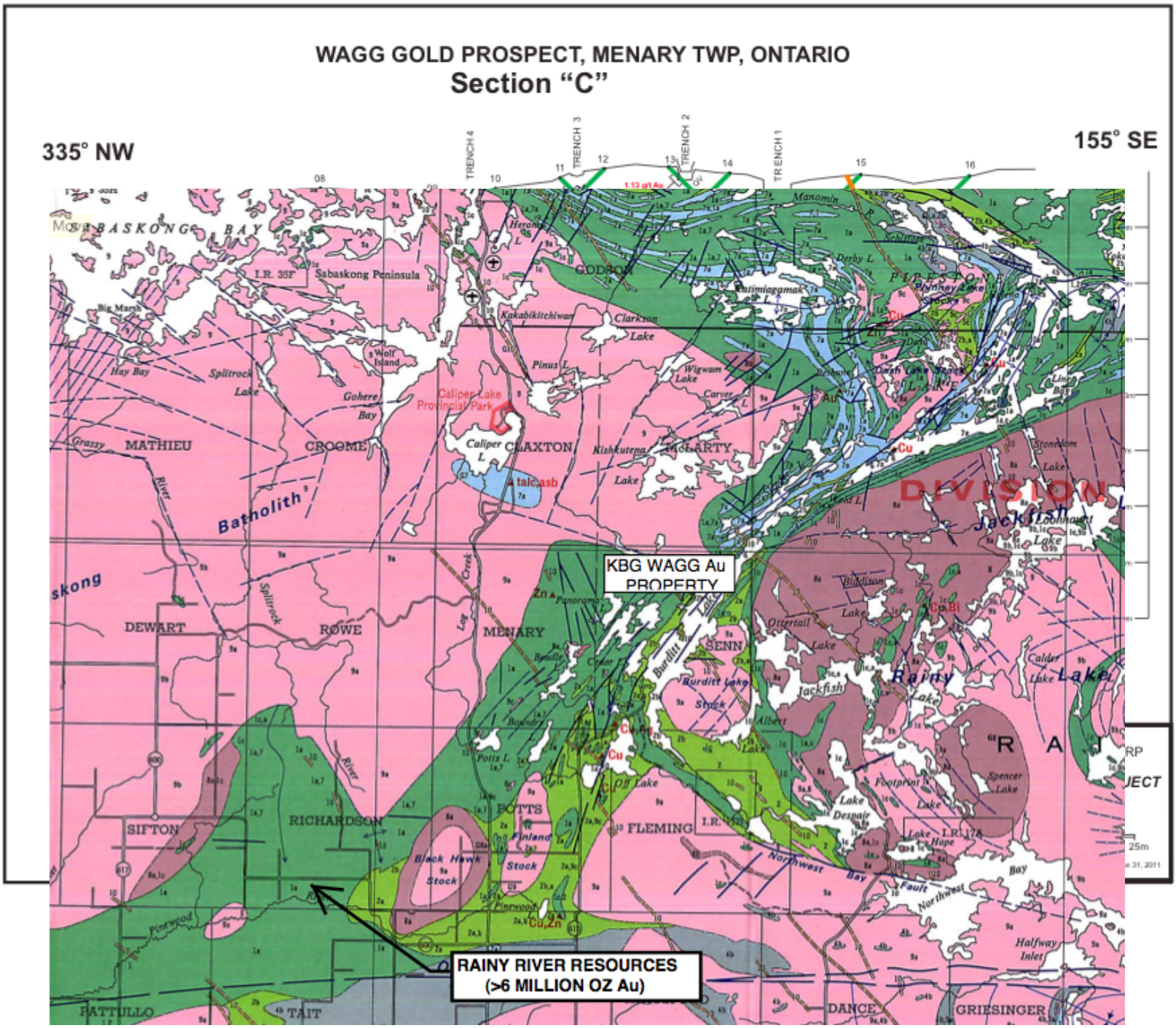

Figure 6: Geological Map depicting the Wagg Prospect and the nearby Rainy River Project.

3.4 Galbraith Prospect

The Galbraith prospect is situated on the immediate batholith contact where Wagg style quartz veins are ubiquitous throughout mafic volcanic host rocks. Drilling at Galbraith intersected a coarse marginal granodiorite phase of the Sabaskong batholith. At Galbraith, non-porphyritic aplitic-syenitic-pegmatitic dykes inject host volcanics. Black quartz veins allowing us to determine relative timings between the host rock, quartz veination and porphyry injections. In addition to Wagg style sugary white quartz, cryptocrystalline black quartz accompanies patchy pegmatite development. This suggests that the genesis of the black cryptocrystalline quartz may be tied to pegmatite melt. These black cryptocrystalline quartz veins also weather orangish-red/cherry red colour, indicating very fine-grained pyrite.

Chapter 4 – Methods

The Menary and Galbraith hand samples represent fresh and calc-silicate altered mafic volcanics, felsic porphyry dykes, biotite altered mafic volcanics, and pyrite bearing quartz veins (Appendix A). The Galbraith samples also included marginal granodiorite and brown mylonite.

Twenty-four core and hand samples were selected to represent various lithologies, 14 from the Wagg drill site and 10 from the Galbraith drill site. Eighteen polished thin sections were made for petrographic analysis. The same 18 samples were submitted to determine bulk rock compositions of major and trace elements combined by XRF and ICP-AES methods. Accurassay Laboratories, based in Thunder Bay, Ontario, was employed to conduct the XRF and ICP-AES analyses. XRF was conducted to analyze major oxides of Si, Al, Ca, K, Mg, Mn, Ti Na, P, Fe and Cr.

Petrographic analysis of thin sections was carried out using a Leica petrographic microscope with transmitted and reflected light capabilities. Petrographic descriptions with estimated modal percentages are provided. Pertinent deformational textures and degree of prograde/retrograde overprinting are documented. Photomicrographs were taken on the Nikon Eclipse LV 100 POL with an attached Nikon DS-Ri1 Digital Sight for computer link up.

The determination of 27 major and minor elements was made by XRF (X-Ray Fluorescence Spectrometer). Sample preparation for XRF analysis by the pressed powder method involved manual crushing of the hand samples and pressing it into fine powdered samples. This technique is prone to analytical uncertainties due to the particle size and

matrix effects of the pressed powders. Trace elements (< 1000ppm) were measured by ICP-AES.

Electron microprobe analyses were employed to characterize metamorphic and hydrothermal mineral species. Renaud Geological Consulting Ltd. performed electron microprobe work for this study using a JEOL JXA-733 electron microprobe with WDS and EDS capabilities. Mineral plots of amphiboles, plagioclase, pyroxene, epidote, and garnets were supplied. Graphs depicting total alkalis vs. tetrahedral Al were supplied for white mica classification.

Chapter 5 – Petrography

5.1 Introduction

Eighteen polished thin sections were made from representative hand and core samples of host rock lithologies as well as gold-bearing quartz veins. Petrographic descriptions of host amphibolitic volcanics, altered lithologies, intrusive lithologies and annealed veins are presented below.

5.2 Amphibolitic Pillow Basalts

Amphibolitic pillow basalt is the dominating lithology at both the Wagg and Galbraith prospects. The pillow basalts are fine grained and dark green in colour. At the site of gold mineralization, the pillow lavas are strongly injected by a variety of porphyry dikes and show calc-silicate bleaching and biotite alteration. Pyrite is common in the biotitized selvages to quartz veins.

The typical modal percentage of fresh amphibolite is 80% hornblende, 15% plagioclase and 5% overgrowing crystalline epidote saussuritized plagioclase clusters. Subidioblastic hornblende ranges from 1-4mm in size forming a fine-grained matrix. Glomeric clusters of plagioclase range from 0.2-0.5mm, these may result from the recrystallization of varioles.

a)

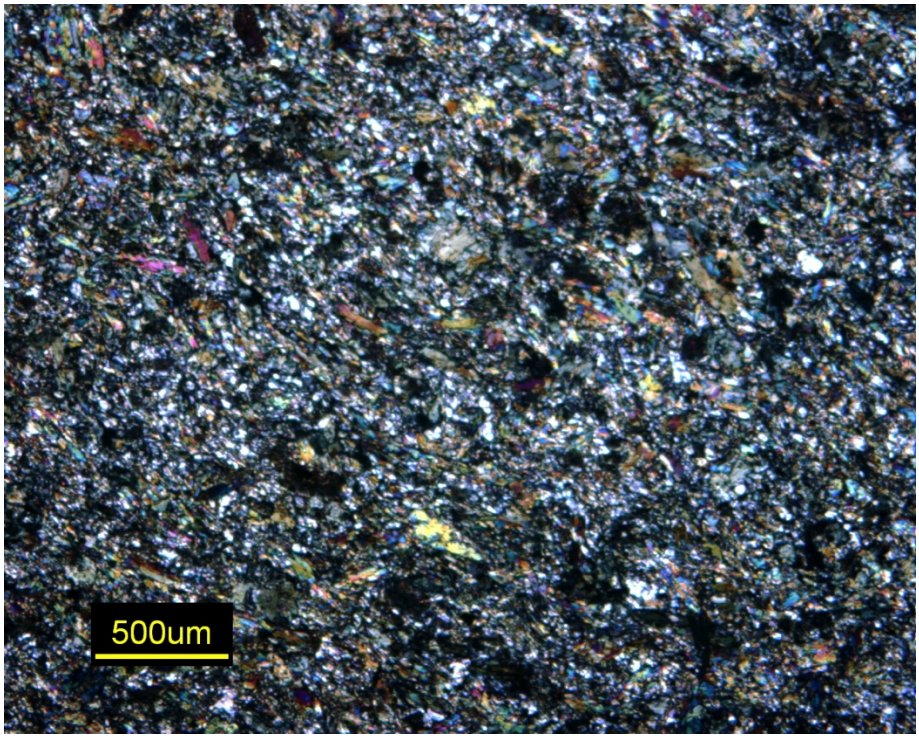

b)

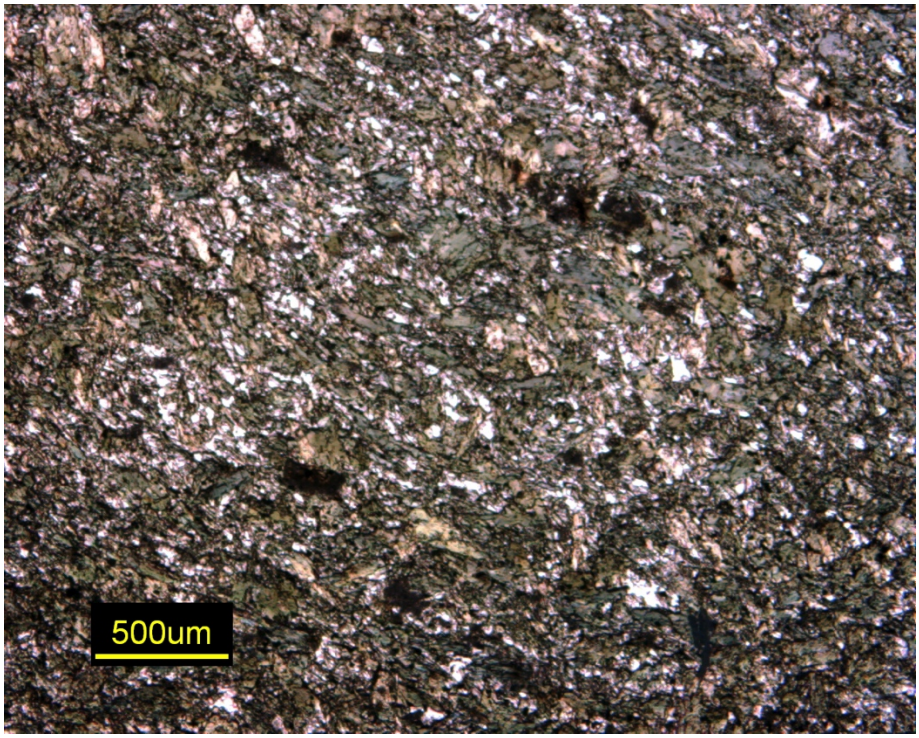

Plate 1: Typical dark green pillow basalt with crystalline epidote in a ground mass of hornblende and plagioclase in a) XPL and b) PPL, from sample thin section Min-21-5.

c)

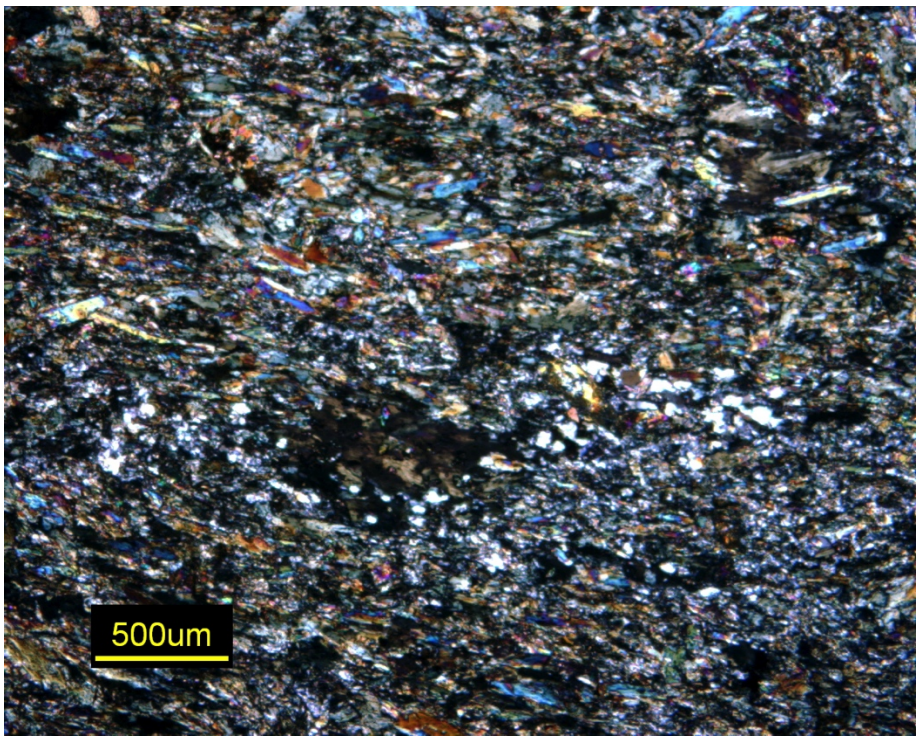

d)

Plate 2: Brown biotite is observed in well foliated amphibolite, plagioclase is replaced by crystalline epidote in c) XPL and d) PPL from thin section Min-21-2.

Figure 7: Located at the Galbraith Prospect. Typical amphibolite injected by a porphyry dyke to the left and quartz vein with biotite-pyrite selvage to the right. Rock hammer for scale.

5.3 Felsic Porphyry Dykes

The amphibolite pillow basalt both at the Galbraith and Menary drill site are strongly injected by intermediate to felsic porphyry dykes up to 3ft in thickness. High strain domains developed along dyke margins host crack-seal type gold-bearing quartz veins.

Figure 8: Feldspar porphyry dyke intruding amphibolitic pillow basalt at Galbraith drill site. Person for scale.

The phaneritic porphyry dykes observed at the Galbraith prospect contain abundant plagioclase in the groundmass and as phenocrysts. These dykes contain plagioclase, epidote, and sericite. The fine-grained groundmass (<1mm) of the plagioclase porphyry dykes is composed of polygonal plagioclase. Recrystallization has thermally annealed the groundmass. White patches occurring in hand samples are due to glomeritic clusters of plagioclase (<1mm), possibly originating as cognate inclusions, and distributed throughout the groundmass. Clusters of crystalline epidote (<1mm) overgrow

the plagioclase grains (~1mm). Large zoned (1-2mm) subhedral phenocrysts of plagioclase contain calcium-rich cores and sodium-rich rims.

Mylonite, intersected at the Galbraith drill site is considered due to dyking into an active deformation zone. This annealed mylonite contains almost no quartz, and is dominated by strongly sericitized potassium feldspar with minor, 5%, disseminated pyrite.

5.4 Quartz Veins

The Wagg prospect consists of a set of en-echelon veins sited proximal to pink-brown weathering feldspar porphyry dykes (Figure 5). At the Galbraith prospect, quartz veins are sited on the immediate batholith/aureole contact where drilling intersected a coarse marginal granodiorite.

The red hematite-stained quartz veins range from stringers of 1cm to about 1m in thickness. Original black-grey pyrite-bearing-quartz veins turn deep cherry red on weathering. In thin section the quartz veins are heteroblastic polygonal with annealed grains up to 400um. Grain boundaries are strongly sutured indicating post emplacement deformation during thermal recrystallization.

a)

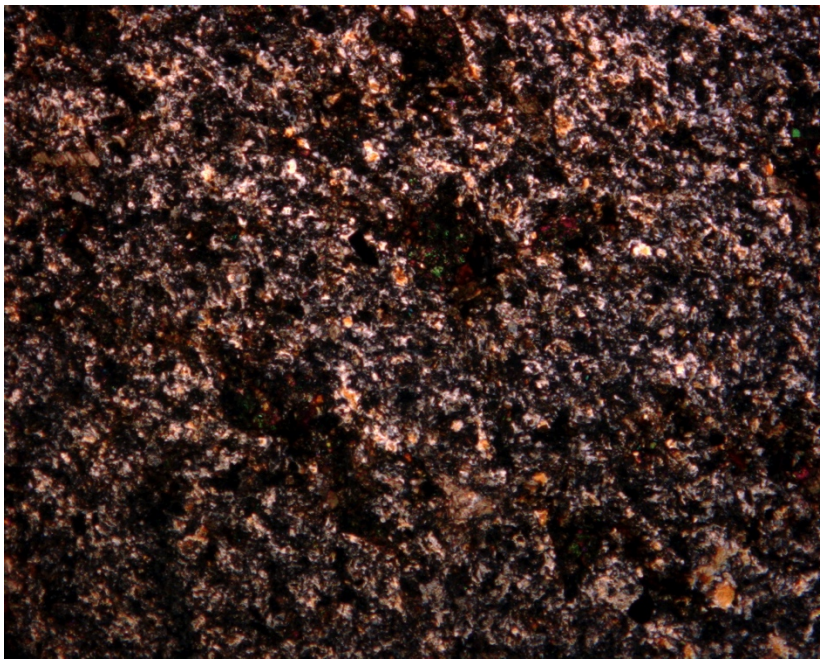

b)

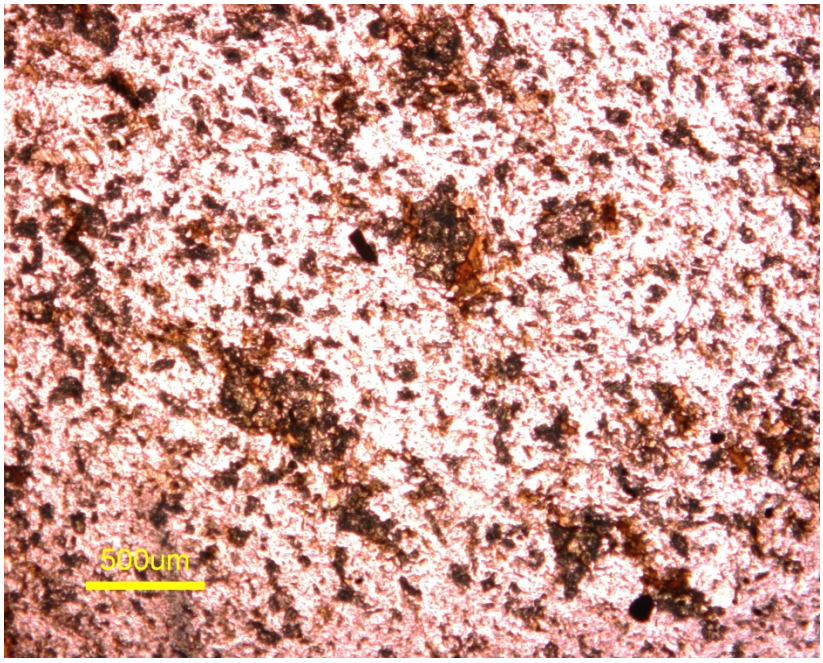

Plate 3: Photomicrographs of feldspar porphyry dyke in a) XPL with glomeritic clusters of plagioclase overgrown by crystalline epidote and in b) PPL from thin section Min-21-4.

c)

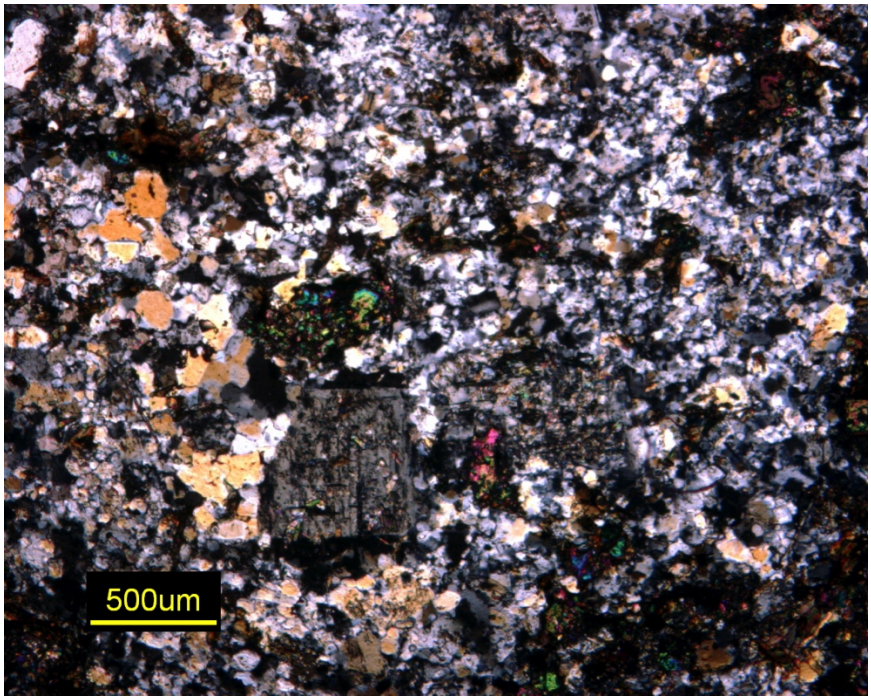

d)

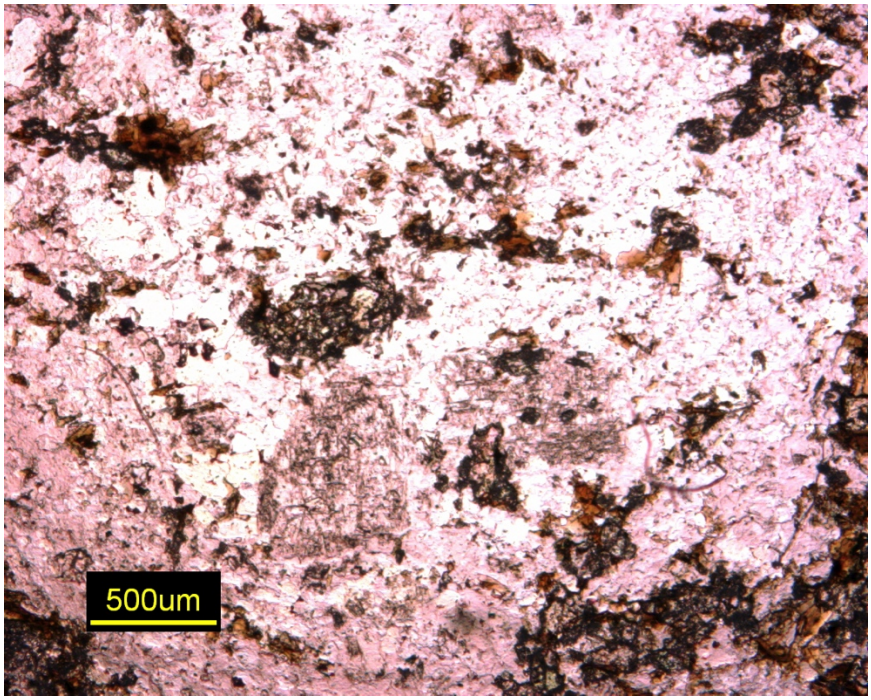

Plate 4: Photomicrographs of porphyry dyke and large hornblende phenocryst taken from Galbraith drill site in c) XPL and d) PPL from thin section Gal-6.

a)

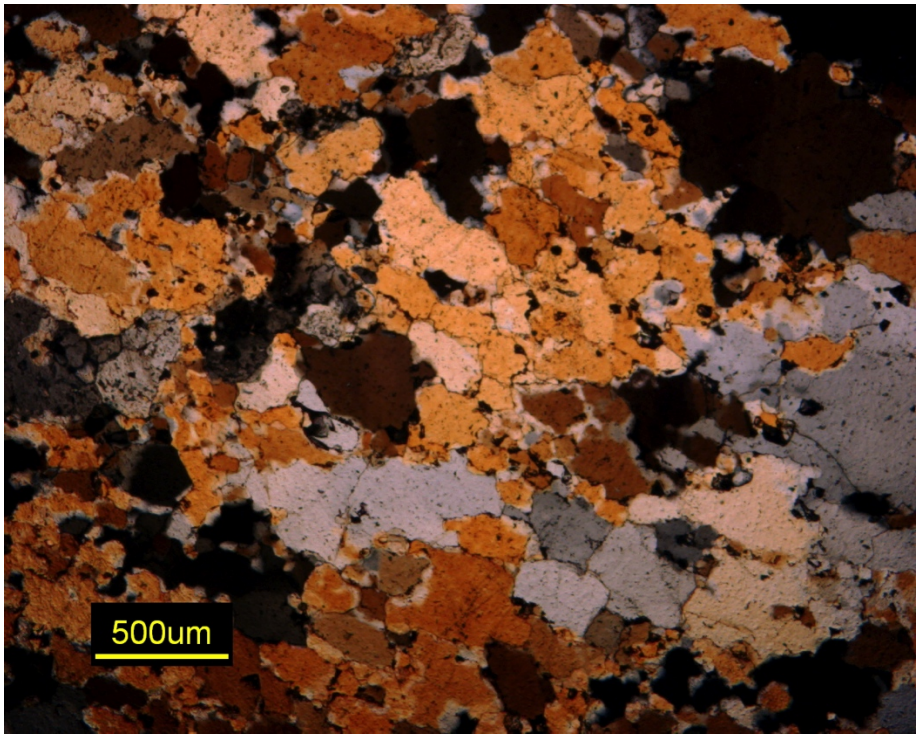

b)

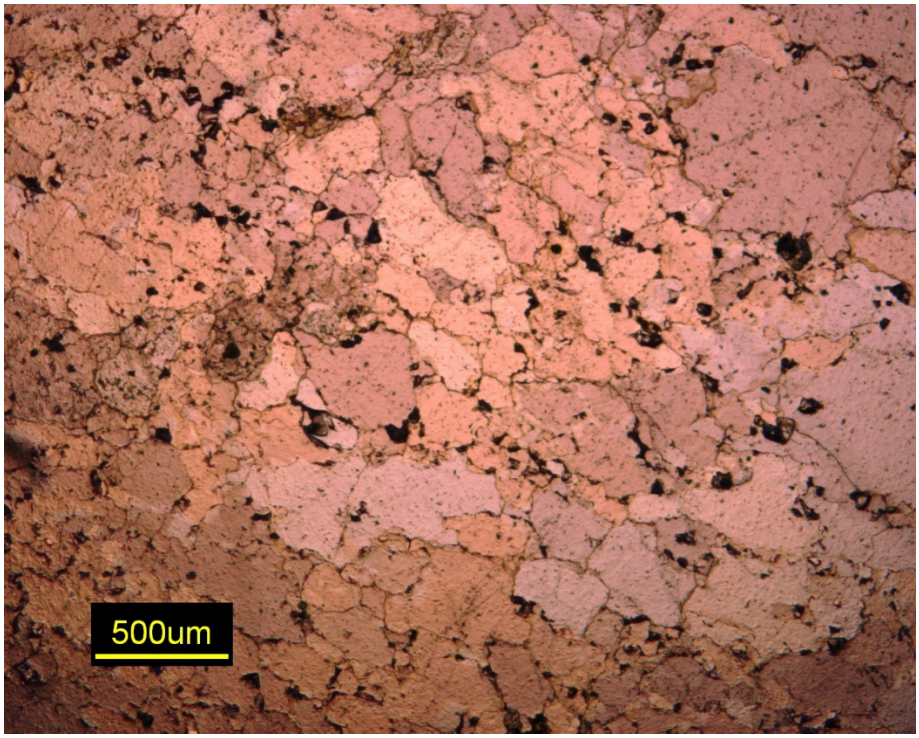

Plate 5: Typical euhedral polygonal quartz with sutured grain boundary found as quartz veins at the Galbraith drill site in a) XPL and b) PPL from thin section Gal-3.

5.5 Pervasive Calc-Silicate Bleaching

Pervasive calc-silicate flooding overprints the amphibolitic pillow basalts at both the Wagg and Galbraith prospects. In calc-silicate altered domains, sheets of coarse, bluish, actinolite (1-2mm) define shear fabric. Where present, biotite is an alteration of the actinolite.

Thin section Gal-5 shows the transitional boundary from fresh amphibolite into the bleached calc-silicate assemblage. The sample is separated into three distinct domains ranging from a typical amphibolite into a bleached domain, up to a reaction front against pegmatite. Microprobe analyses show the amphibolite is dominated by hornblende. Decussate hornblende is intergrown with xenoblastic plagioclase forming the interstices

to idioblastic hornblende. Alignment of the decussate hornblende gives rise to a moderate fabric. In this bleached domain, plagioclase is pervasively saussuritized to epidote. Calcium metasomatism results in forming colorless actinolite (1-2 mm). At the reaction front between the pegmatite and calcsilicate altered amphibolite, the original amphibolite texture is completely destroyed. Polygonal grains of crystalline epidote (<1mm to 2mm) increase in grain size towards the reaction front. Garnet and clinopyroxene is also restricted to the reaction front.

Chapter 6 - Mineral Chemistry

6.1 Introduction

Microprobe analyses were preformed on six polished thin sections. This work focused on determining the specific mineral speciation of amphibole, pyroxene, plagioclase, mica, and garnet. Specific probe locations were chosen during a petrographic study.

The amphibole compositions are plotted as total Alkalis vs Tetrahedral Al with silica in the formula and with sodium and potassium in the formula (Figure 9). The pyroxenes are plotted on a Wollastonite-Enstatite-Ferrosilite ternary diagram (Figure 10). Plagioclase was also plotted on an Orthoclase-Albite-Anorthite ternary diagram as well as micas (Pyralspite-Grossular-Andradite) (Figure 11 & 12). Plotted on a classification diagram, micas are plotted as total Al vs. Mg/Fe (Figure 13).

6.2 Microprobe analysis of Amphibole

Amphibole data was plotted on a total alkali vs. tetrahedral Al graph (Figure 9). Amphibole within the pillow basalts ranges from ferrohornblende where fresh to magnesiohornblende to actinolite with increasing calc-silicate bleaching. A complete spectrum of crystal chemistry is observed ranging from near zero aluminum in actinolites to one fourfold Al in ferrohornblende.

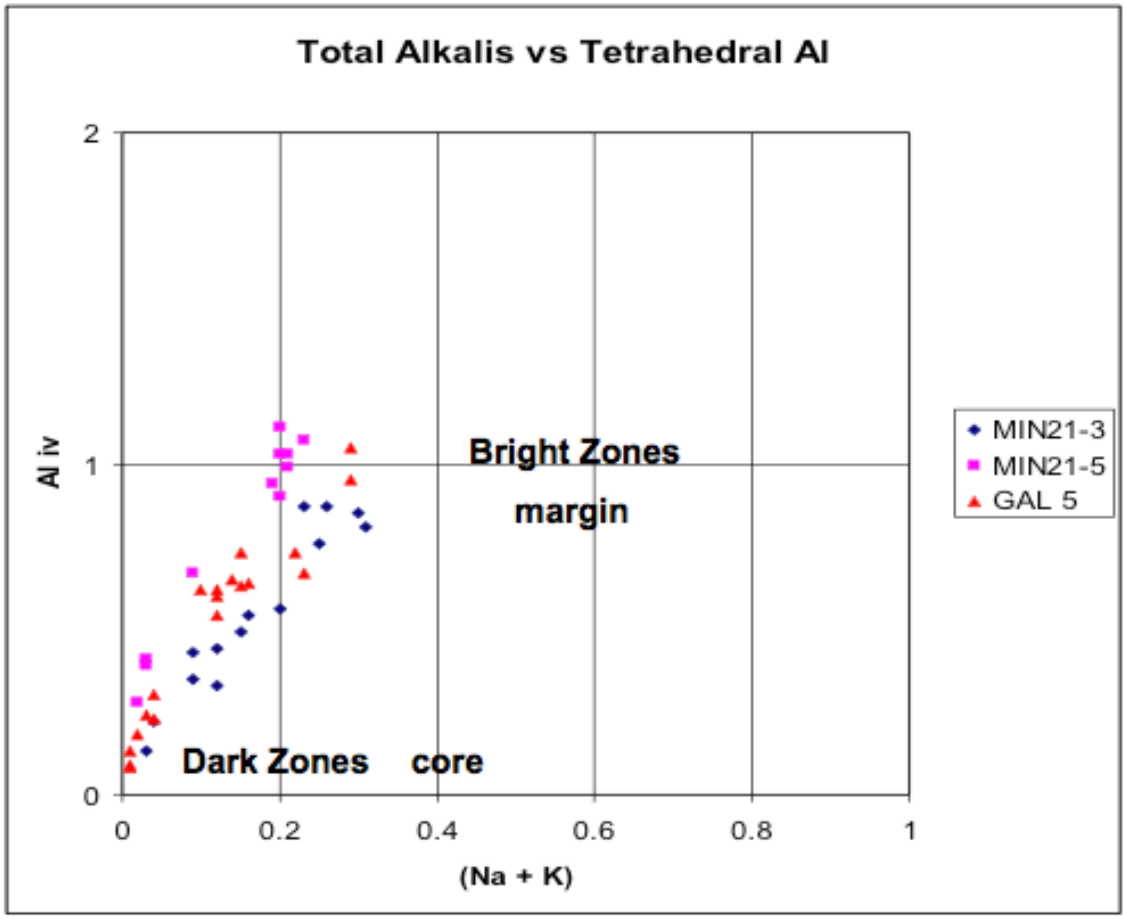

Figure 9: Plot of Alkalis vs. Tetrahedral Al in amphiboles from iron tholeiites.

6.3 Microprobe analysis of Pyroxene

Pyroxene only occurs at the metasomatic front developed between calc-silicate flooded amphibolite and pegmatite. The pyroxene is intermediary between diopside and hedenbergite in composition (Figure 10). Diopside is a monoclinic pyroxene with a chemical formula of MgCaSi2O6. Hedenbergite (CaFeSi2O6) forms a solid solution with diopside and is the iron rich end member of this pyroxene group.

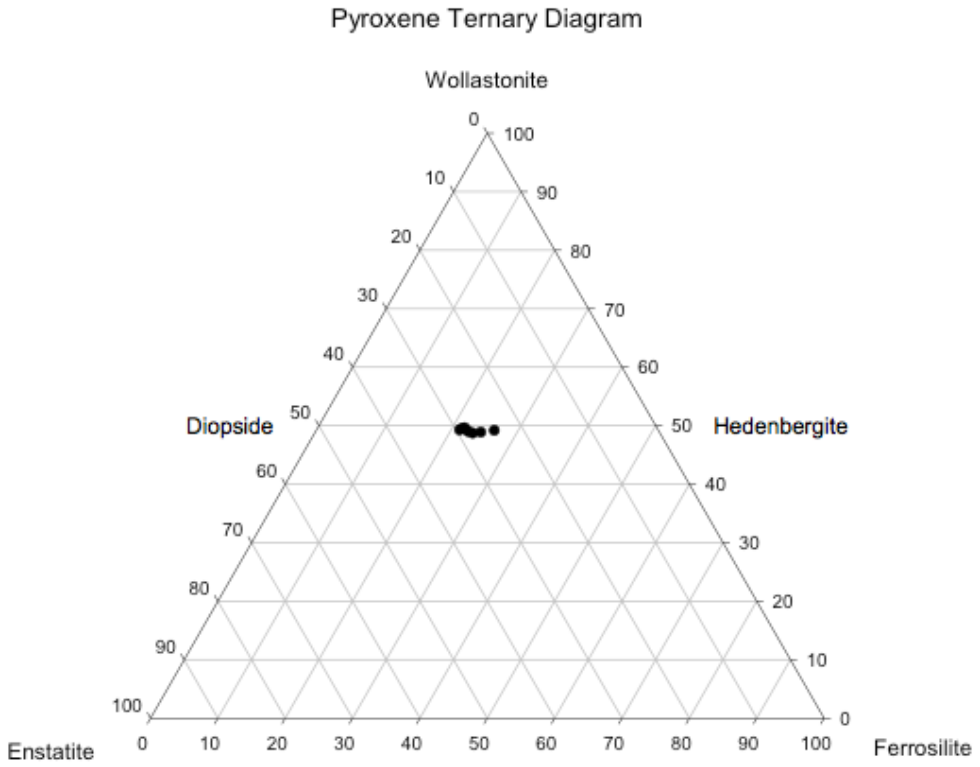

Figure 10: Ternary diagram depicting pyroxene end member compositions.

6.4 Microprobe analysis of Feldspar

Forty-six determinates were conducted on various felsic feldspar porphyry dykes from Menary and Galbraith prospects. These were plotted on a plagioclase/feldspar end member ternary diagram (figure 11). Results report potassium feldspar only occurs in sample Gal-9, considered a mylonite dyke rock. The typical porphyry dykes have growth-zoned phenocrysts ranging from core andesine to rim oligoclase. The plagioclase composition suggests a melt fractioning from andesite to dacite over the course of growth of plagioclase phenocrysts.

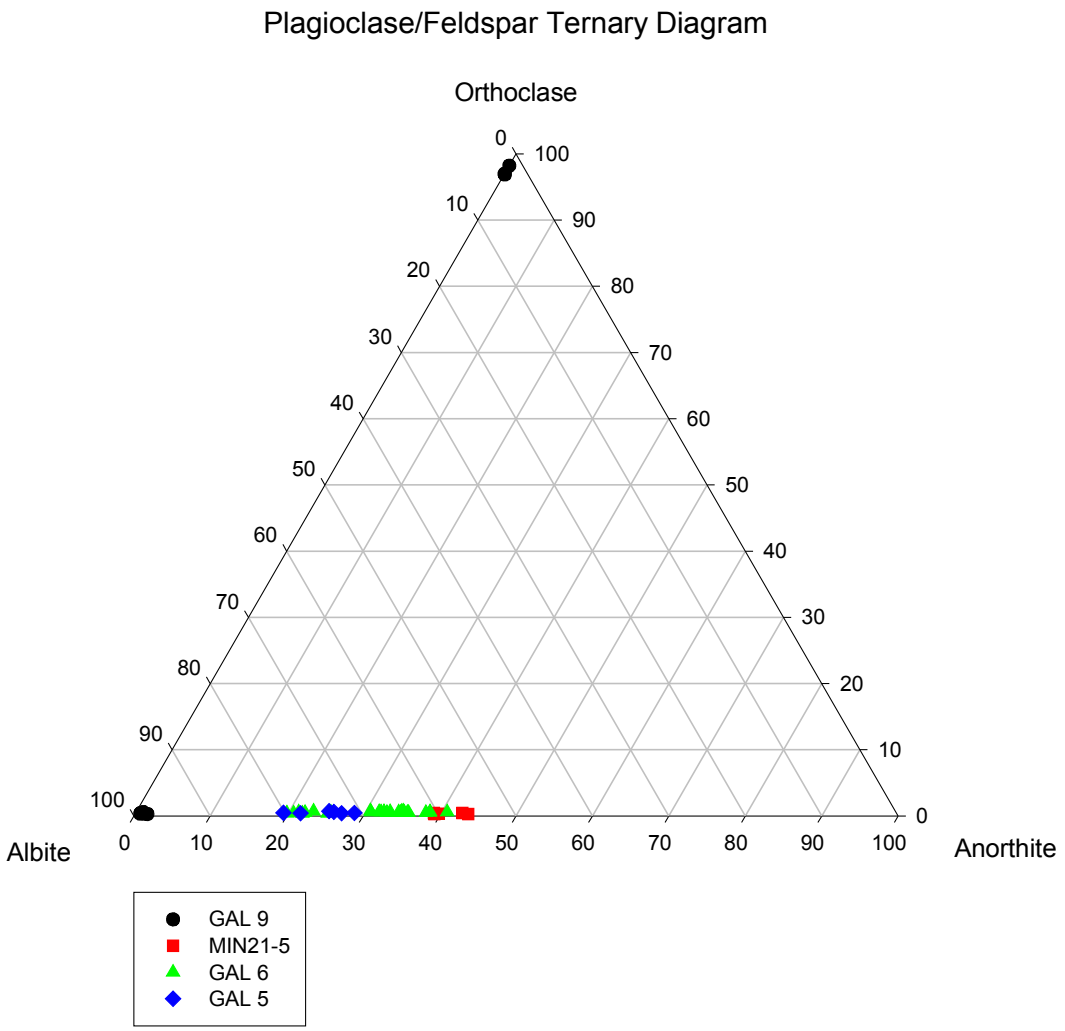

Figure 11: Ternary diagram depicting plagioclase/feldspar end member compositions.

6.5 Microprobe analysis of Micas

Sixteen probe points was conducted on 3 different samples to identify the speciation of white mica. The results are plotted on a mica classification diagram defined on the basis of total aluminum versus Mg/Fe ratios. The white mica at the Galbraith and Menary has high Al, low Mg/Fe, forming high iron phengite.

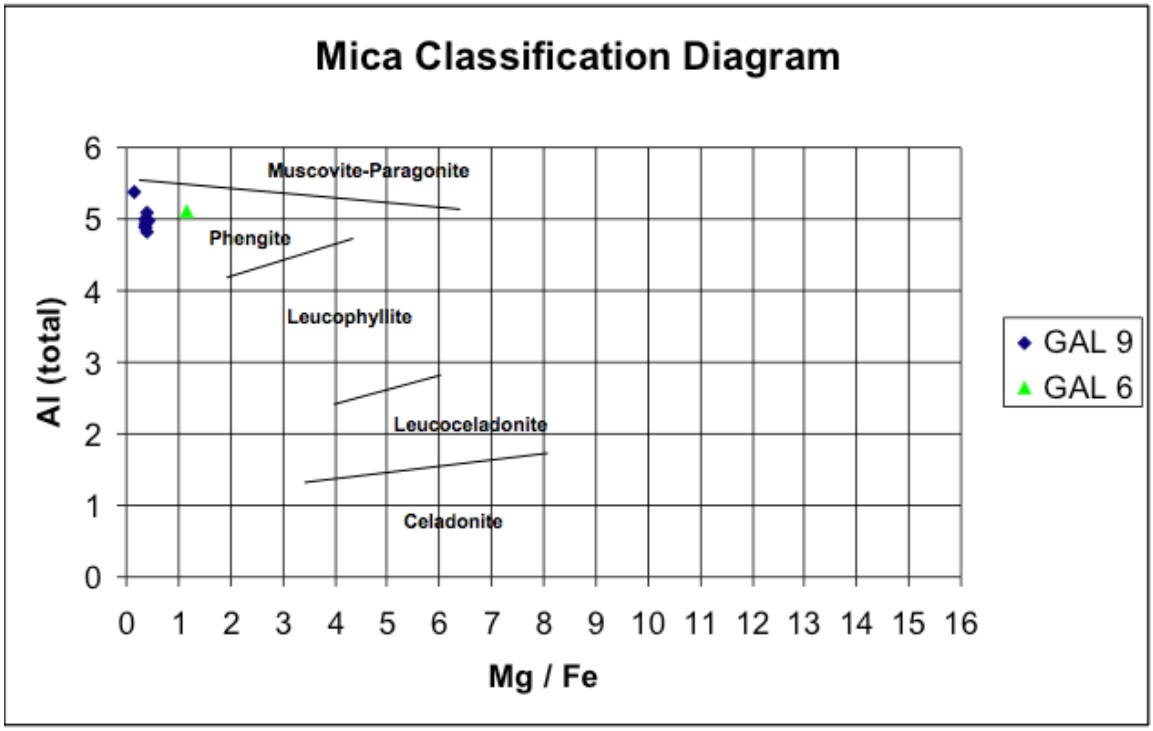

Figure 12: Diagram depicting Mica classification based on total Al vs. Mg/Fe ratios.

Biotite, found at the Wagg and Galbraith prospects, is characterized by a Fe/Me ratio of around 1 (Figure 13), characteristic of the host basalt. Biotite occurs as a restricted alteration product found along shear zones between the quartz selvages.

6.6 Microprobe analysis of Garnet

Garnet only occurs at the reaction front of calcsilicate bleaching amphibolite and pegmatite. Plotted on a ternary end member diagram, the garnet at the Galbraith prospect is close to a grossular end member with the chemical composition of Ca3Al2Si3O12. Grossular is the calcium-aluminum mineral species of the garnet group.

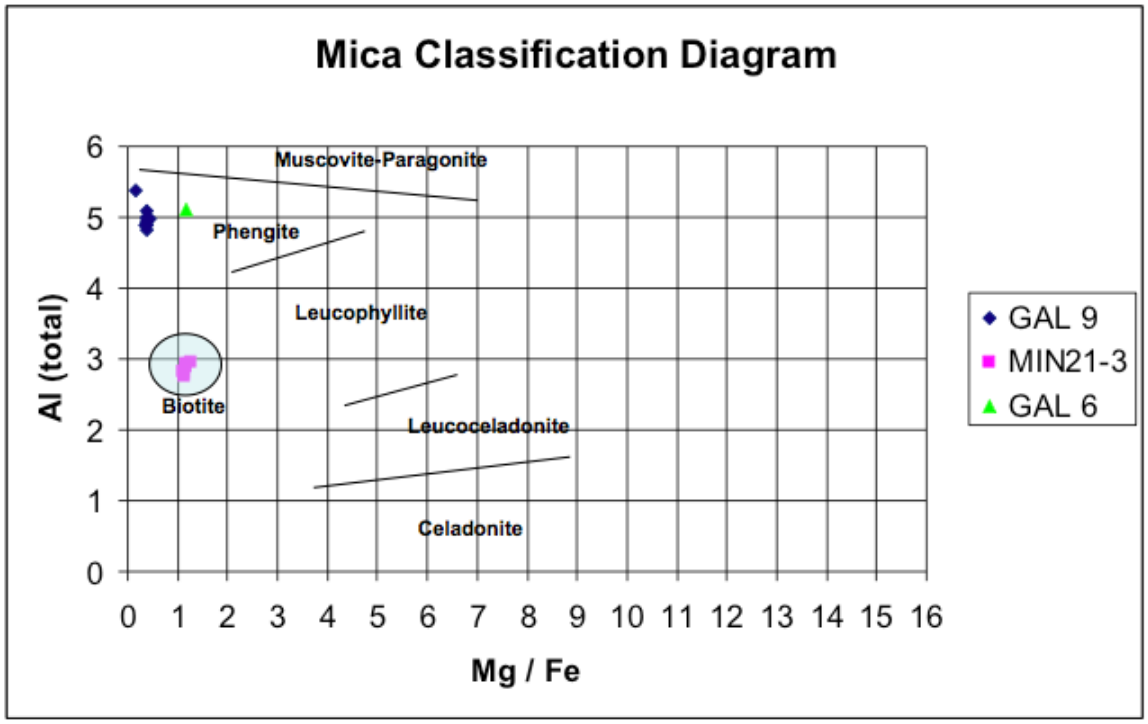

Figure 13: Diagram depicting Mica classification based on total Al vs. Mg/Fe ratios with biotite included.

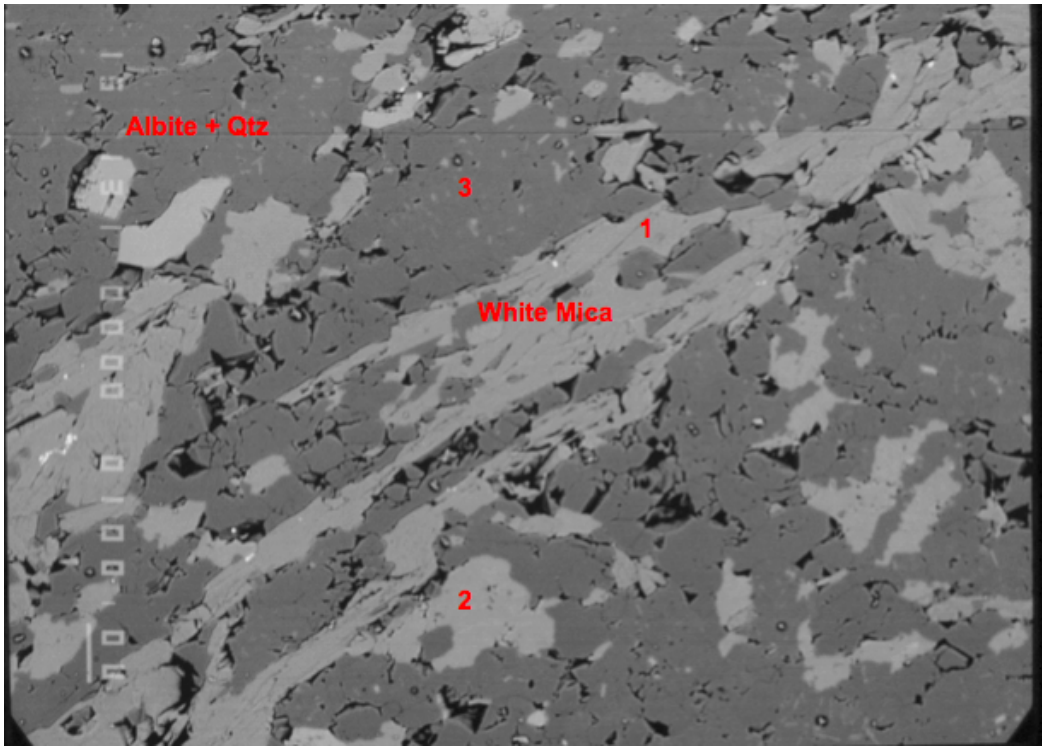

Plate 6: Total Field of View: 10 mm. Backscatter image of white mica at points 1 & 2, albite and quartz at point 3.

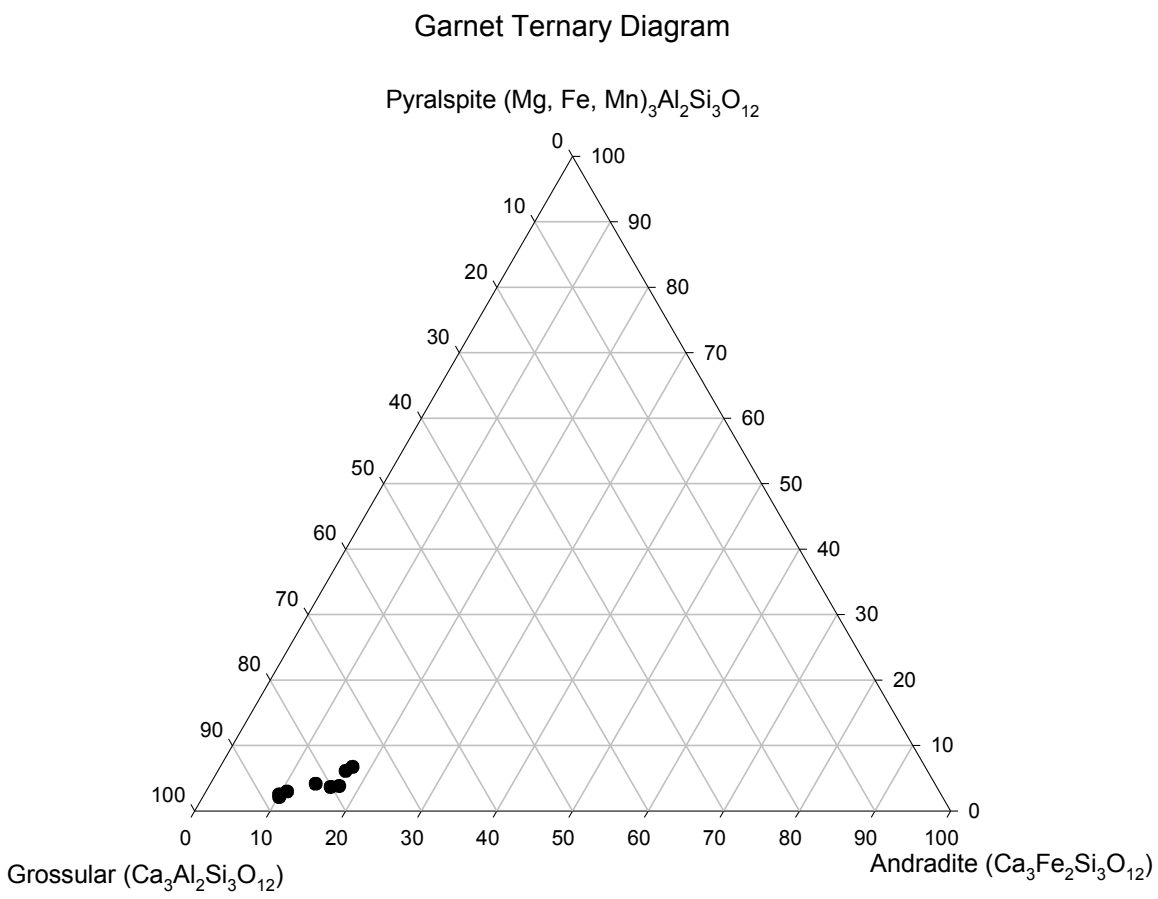

Figure 14: Ternary diagram depicting garnet end member compositions.

Chapter 7 - Bulk Rock Geochemistry

7.1 Introduction

Limited bulk rock geochemistry was carried out on both fresh and altered amphibolitic pillow basalts as well as porphyry dykes. The combined XRF and ICP-AES results characterized the major, minor, and trace element abundances within various lithologies.

7.2 Bulk Rock Analysis of Major and Minor Element Geochemistry

The following results are shown in Appendix C Table 1.

Samples Gal-4, 5 and Min 21-1,2,5 represent fresh iron tholeiitic basalt from the Galbraith and Wagg prospects respectively (Table 1). Sample Gal-5 represents amphibolite that has been calc-silicate altered. Si contents of the amphibolites range from 47-53% SiO_2. The total iron content ranges from 11 to 17% Fe_2O_3, indicating a very high iron content within the original basalt. Titanium levels of 0.7-1.4%, are characteristic of iron-rich tholeiite. Where Gal-5 has undergone calc-silication, loss of iron is coupled with a gain in calcium. Relatively high phosphorus and magnesium contents in the fresh amphibolite are also depleted in zones of calc-silicate bleaching.

Samples Gal-6, 8 and Min 21-4 represent felsic porphyry dykes that intrude the pillow lavas. Analyses of major elements show total SiO_2 contents range from 61-69%. Sodium contents of the felsic dykes are on average 5% but potassium contents are generally below 1.5%.

Sample Gal-10 represents the granodiorite that borders the with pillow basalts at the Galbraith prospect. It has similar silica content as the felsic porphyry dykes and total sodium and potassium contents are 5% and 1.4% respectively. Gal-9 (Na/K ratio of 1) likely represents a mylonitic dyke rock of a more evolved composition. Highly silicate, 76% of total composition is SiO_2. The rich rock represents an intrusion into an active deformation zone that has been strongly K-metasomatised.

7.3 Bulk Rock Analysis of Trace Element Geochemistry

The following results are shown in Appendix C Table 2.

ICP analyses of the amphibolitic pillow basalts show consistent elevation in Mn, P, Ti and V. Sample Gal-5 represents a calc-silicate overprinted amphibolite that contains 1120 ppm of Mn. As well phosphorus ranges from 293ppm to 689ppm, titanium ranges from 2413 to 3590 ppm. Vanadium ranges from 71-158 ppm. The elevated abundance of these trace elements was inherited from the Fe-tholeiitic parent rock.

ICP analyses of felsic porphyry dykes, samples Gal-6, 8 and Min 21-4, contain up to 100-200 ppm of trace chromium. Gal-8 represents a non-altered porphyry dyke that contains 548 ppm of Cr, in contrast, altered dyke Gal-6 contains 259 ppm. This suggests the high Cr background of dykes in inherited from the original melt.

Gal-10, representing the marginal granodiorite phase of the Sabaskong Batholith at Galbraith prospect contains up to 287 ppm of Cu, 118 ppm Pb and tungsten at 346ppm. This identifies a substantially different trace element signature than the marginal dykes.

Chapter 8 – Discussion

The Wagg and Galbraith gold prospects are plutonic in setting, occurring in the thermal aureole of the Sabaskong Batholith. Host rock mafic pillow basalts, at both prospects, are overprinted by amphibolite facies metamorphic conditions at 500-600°C and 0.2-1.2 GPa (Winter, 2011). Bulk rock geochemistry demonstrates high iron contents that range from 11 to 17% Fe_2O_3 and titanium levels of 0.7-1.4%. Inheritance of mineral chemistry from parent rock iron tholeiites explains the high presence of iron as shown in bulk rock data.

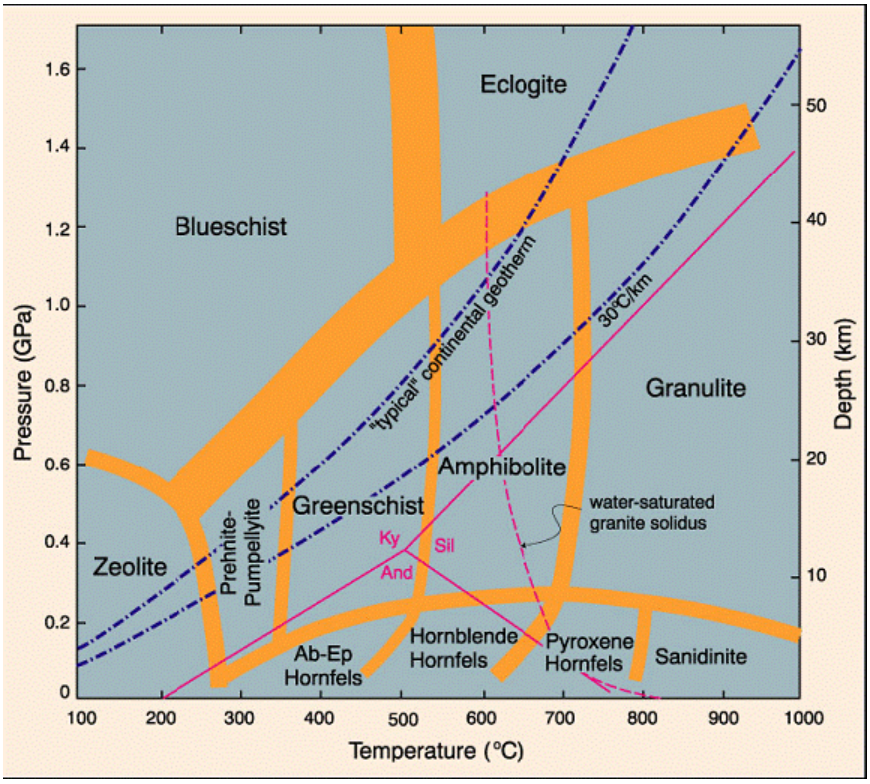

Figure 15: Metamorphic facies diagram depicting temperature-pressure zones. Transitional zones are depicted as orange lines (Winter, 2001).

Amphibolitic pillow lavas found at both prospects show conjugate jointing and local ductile shearing. Petrographic analysis along with electron microprobe data suggests that the hornblende-plagioclase assemblage underwent metasomatic calc-silicate bleaching at 500-600°C under high CO_2 partial pressures (Winter, 2001) (Figure 15). Microprobe analyses of amphiboles indicate that the amphibole within the pillow basalts ranges from ferrohornblende where fresh to magnesiohornblende to actinolite with increasing calc-silicate bleaching.

Calc-silicate flooding (actinolite-epidote-plagioclase) occurred as the system began to cool, pervasive calc-silicate alteration suggests high temperature CO_2 degassing through the aureole of the batholith. Microprobe analysis of Grossular garnet and hedenbergitic pyroxene suggests near peak temperature conditions. Detailed petrographic study shows the reaction front between a calc-silicate domain and host amphibolitic pillow basalt. In calc-silicate altered domains, sheets of coarse, bluish, actinolite (1-2mm) define shear fabric. Crystalline epidote forms as a result of saussuritization of plagioclase at the reaction front. Here, the original amphibolitic texture is completely destroyed.

A series of intermediate to felsic porphyry dykes inject the pillow basalts at the Wagg and Galbraith prospects, post dating the calc-silication. Electron microprobe analyses of plagioclase phenocrysts indicate the aureole was invaded by fractionating andesite to dacitic melts. The same analyses concluded that the felsic porphyry dykes were albitic in composition. Mineral chemistry shows a high Cr content up to 548 ppm.

Brittle to ductile deformation due to strain from the aureole of the Sabaskong Batholith formed aligned shears in rocks at the Wagg and Galbraith prospects. Biotitization of these shears occurred during retrograde reactions at mid-greenschist

conditions, <450°C (Winter, 2001). Hydrothermal remobilization of Au during subsequent retrograde cooling concentrated free gold and sulphides in quartz veins. Shear zones of the high strain domains hosts the gold bearing quartz veins in a crack-seal style mineralization.

Chapter 9 - Conclusion

The results of this study is summarized below:

1. The Wagg and Galbraith prospects are hosted in iron-rich tholeiitic basalt occurring in the amphibolite facies aureole of the Sabaskong Batholith. Bulk rock geochemistry indicates high levels of Mn, P, Ti and V.

2. Petrographic evidence along with mineral chemistry demonstrates that the pillow basalts in the contact aureole of the Sabaskong batholith have undergone prograde metamorphism subjecting it to amphibolite facies metamorphic conditions (500-600°C and 0.2- 1.2Gpa).

3. Calc-silicate flooding occurred as the system began to cool, suggesting high temperature CO_2 degassing at the batholith margin.

4. A series of felsic porphyry dykes intrude the host pillow basalts near peak metamorphic conditions.

5. Strain in the aureole of the Sabaskong batholith formed brittle to ductile shears. Limited biotitization of sheared domains occurred at mid greenschist facies conditions (450-400°C).

6. Hydrothermal remobilization of Au during retrograde cooling concentrated free gold in quartz veins developed both interior and exterior to dyke margins.

References

Blackburn, C.E., 1976, Geology of the Off Lake – Burditt Lake Area, District of Rainy River; Ontario Division of Mines Geoscience Report 140, p. 62.

Blackburn, C.E. and Wagg, Geological Setting of Gold, Western Wabigoon Subprovince, Canadian Shield: Exploration Targets in Mixed Volcanic Successions, NRC Research Press, 2075 p.

Card, K.D., 1990. A Review of the Superior Province of the Canadian Shield, a product of Archean accretion: Precambrian Research, v. 48, p. 99.

Hall, D.H. Crustal Magnetization Beneath the Aulneau and Sabaskong Batholiths, Kenora and Fort Frances districts, Ontario, Canada, 61 p.

Holmstead, W.E and Wagg. 1993, 1992 Exploration Programme on the Menary Township Property, District of Kenora, Ontario, Western Troy Capital Resources Inc.: Kenora, Assessment Files, Kenora Ministry of Northern Development and Mines, 142 p.

Kwong, Y.T.J. and Crocket, J.H., 1978, Background and Anomalous Gold in Rocks of an Archean Greenstone Assemblage, Kakagi Lake area, northwestern Ontario: Economic Geology, v. 73, p. 50-63.

Mareschal, J.C. and Jaupart, C., 2004, Variations of Surface Heat Flow and Lithospheric Thermal Structure Beneath the North American Craton: Earth and Planetary Science Letters, v. 223, p. 65-77.

Ontario Ministry of Natural Resources, 1982, Geology of the Straw Lake Area Districts of Kenora and Rainy River.

Ontario Ministry of Natural Resources, Beard, R.C. and Garratt, G.L., 1971, Gold Deposits of the Kenora-Fort-Frances Area - Districts of Kenora and Rainy River. (Rep.1984).

Ontario Ministry of Natural Resources. Division of Mines and Edwards, G.R., 1980, Geology of the Bethune Lake Area - Districts of Kenora and Rainy River.

Ontario Ministry of Natural Resources. Division of Mines, Beard, C.R., Garratt, G.L. and Ontario. Ministry of Natural Resources, 1971, Gold Deposits of the Kenora-Fort Frances Area: Districts of Kenora and Rainy River.

Percival J A., Sanborn-Barrie M., Skulski T., Stott G M., Helmstaedt H., White DH, , Tectonic Evolution of the Western Superior Province from NATMAP and Lithoprobe studies, NRC Research Press, 1085 p.

Rolandone, F., Mareschal, J.C., Jaupart, C., Gosselin, C., Bienfait, G. and Lapointe, R., 2003, Heat flow in the Western Superior Province of the Canadian shield: Geophysical Research Letters, v. 30, p. 1637.

S.C., S., 1988, Genesis and Evolution of the Ore Deposits in the Early Precambrian Greenstone Belts and Adjacent High Grade Metamorphic Terrains of Peninsular India — A study in similarity and contrast: Precambrian Research, v. 39, p. 107-130.

Winter, John D. 2001: An Introduction to Igneous and Metamorphic Petrology. Prentice-Hall Inc. Upper Saddle River, New Jersey.

Appendix A: Hand Sample Classification

Min-1	Biotitized Mafic Volcanics
Min-2	Quartz Vein
Min-3	Quartz Vein from Vein A
Min-4	Quartz Vein from Vein B
Min-5	Quartz Vein from Vein B (Wall Rock)
Min-6	Quartz Vein from Vein D
Min-21-1	Calc-silicate Altered Mafic Volcanics
Min-21-2	Pristine Mafic Volcanics
Min-21-3	Calc-silicate Altered Mafic Volcanics
Min-21-4	Porphyry Dyke
Min-21-5	Pristine Mafic Volcanics
Min-22-1	Porphyry Dyke at 44', margin to high grade qtz vein 57g/ton.
Min-22-2	Mafic Volcanics
Gal-1	Mafic Volcanics
Gal-2	Quartz Vein
Gal-3	Quartz Vein
Gal-4	Pristine Mafic Volcanics
Gal-5	Pegmatitic Fluids juicing Mafic Volcanics
Gal-6	Porphyry Dyke at 477' Flanked by

	Mafic Volcanics 5' back
Gal-7	Quartz Vein
Gal-8	Porphyry Dyke
Gal-9	Brown Mylonite
Gal-10	Granodiorite

Appendix B: Mineral Chemistry From Microprobe Analysis

In order of Amphiboles, Plagioclase, Pyroxene, Epidote, Mica, and Garnets

AMPHIBOLE, RODERICK TOM-YING, KINGSBAY GOLD CORP., Feb 2012, R.G.C.

	1	2	3	4	5	6	7	8
SIO2	54.12	49.21	48.92	52.05	48.84	51.93	51.26	52.65
TIO2	.06	.08	.16	.06	.15	.07	.04	.13
A2O3	1.28	5.95	6.87	4.76	5.99	4.96	4.65	3.31
C2O3	.02	.09	.01	.00	.00	.00	.03	.03
FEO	13.26	16.97	15.77	13.83	16.69	14.84	14.85	16.06
MGO	16.22	12.92	11.46	13.93	12.62	13.60	13.60	12.71
MNO	.44	.39	.65	.35	.54	.37	.33	.33
K2O	.09	.42	.50	.32	.51	.31	.30	.33
CAO	12.55	12.06	12.05	12.25	12.34	12.31	12.55	12.36
NA2O	.09	.78	.76	.63	.72	.59	.59	.45
BAO	.14	.00	.00	.00	.00	.11	.00	.00
F	.59	.00	.00	.00	.62	.00	.00	.04
CL	.01	.01	.01	.01	.00	.01	.01	.00
SUM	98.87	98.88	97.16	98.19	99.02	99.10	98.21	98.40
-O= F+CL	.25	.00	.00	.00	.26	.00	.00	.02
SUM	98.62	98.88	97.16	98.19	98.76	99.10	98.21	98.38

SI	7.739	*	7.214	*	7.257	*	7.521	*	7.157	*	7.477	*	7.461	*	7.665	*
AL	.216	7.955	.786	8.000	.743	8.000	.479	8.000	.843	8.000	.523	8.000	.539	8.000	.335	8.000
AL	.000	*	.241	*	.458	*	.331	*	.192	*	.319	*	.258	*	.232	*
TI	.006	*	.009	*	.018	*	.007	*	.017	*	.008	*	.004	*	.014	*
CR	.002	*	.010	*	.001	*	.000	*	.000	*	.000	*	.003	*	.003	*
FE	1.586	*	2.080	*	1.957	*	1.671	*	2.045	*	1.787	*	1.808	*	1.955	*
MG	3.457	*	2.823	*	2.534	*	3.000	*	2.757	*	2.919	*	2.950	*	2.758	*
MN	.053	5.105	.048	5.212	.082	5.050	.043	5.052	.067	5.077	.045	5.077	.041	5.065	.041	5.004
BA	.008	*	.000	*	.000	*	.000	*	.000	*	.006	*	.000	*	.000	*
CA	1.923	*	1.894	*	1.915	*	1.896	*	1.938	*	1.899	*	1.957	*	1.928	*
K	.016	*	.079	*	.095	*	.059	*	.095	*	.057	*	.056	*	.061	*
NA	.025	1.972	.222	2.194	.219	2.229	.176	2.132	.205	2.237	.165	2.127	.166	2.179	.127	2.116
F	.267	*	.000	*	.000	*	.000	*	.287	*	.000	*	.000	*	.018	*
CL	.002	*	.002	*	.003	*	.002	*	.000	*	.002	*	.002	*	.000	*
O	23.000	*	23.000	*	23.000	*	23.000	*	23.000	*	23.000	*	23.000	*	23.000	*
FE	31.45		42.43		43.57		35.78		42.60		37.97		37.99		41.48	
MG	68.55		57.57		56.43		64.22		57.40		62.03		62.01		58.52	
F/M	.474		.754		.804		.571		.766		.628		.626		.724	
F/FM	.322		.430		.446		.364		.434		.386		.385		.420	

1 ****MIN21-3 C1 - ACICULAR TREM - SPOT 1 - DK CORE
2 MIN21-3 C1 - ACICULAR TREM - SPOT 1 - BT MARG
3 MIN21-3 C1 - ACICULAR TREM - SPOT 2 - BT DOM
4 MIN21-3 C1 - ACICULAR TREM - SPOT 2 - DK DOM
5 MIN21-3 C1 - ACICULAR TREM - SPOT 3 - BT DOM
6 MIN21-3 C1 - ACICULAR TREM - SPOT 3 - DK DOM
7 MIN21-3 C1 - SPOT 4 - DK DOM
8 MIN21-3 C1 - SPOT 4 - BT DOM

AMPHIBOLE, RODERICK TOM-YING, KINGSBAY GOLD CORP., Feb 2012, R.G.C.

	9	10	11	12	13	14	15	16
SIO2	52.10	52.75	49.03	55.28	52.82	48.84	47.46	47.77
TIO2	.06	.04	.11	.03	.07	.18	.47	.34
A2O3	3.30	3.05	6.35	.97	4.13	7.06	9.11	9.00
C2O3	.00	.00	.09	.07	.04	.00	.08	.14
FEO	16.14	14.16	16.86	12.72	14.51	16.43	18.68	18.48
MGO	13.40	15.02	12.18	16.48	13.07	11.90	10.28	10.38
MNO	.39	.52	.30	.22	.32	.47	.34	.39
K2O	.35	.21	.66	.11	.28	.66	.18	.17
CAO	12.39	12.32	11.70	12.50	12.24	11.85	11.20	11.13
NA2O	.34	.36	.96	.08	.49	.89	1.20	1.12
BAO	.00	.00	.00	.00	.05	.11	.00	.06
F	.53	.00	.50	.00	.11	.03	.00	.00
CL	.00	.00	.00	.00	.00	.00	.00	.00
SUM	99.00	98.43	98.74	98.46	98.13	98.42	99.00	98.98
-O= F+CL	.22	.00	.21	.00	.05	.01	.00	.00
SUM	98.78	98.43	98.53	98.46	98.08	98.41	99.00	98.98

SI	7.556	*	7.616	*	7.194	*	7.881	*	7.643	*	7.183	*	6.982	*	7.019	*
AL	.444	8.000	.384	8.000	.806	8.000	.119	8.000	.357	8.000	.817	8.000	1.018	8.000	.981	8.000
AL	.120	*	.135	*	.292	*	.044	*	.348	*	.407	*	.561	*	.577	*
TI	.007	*	.004	*	.012	*	.003	*	.008	*	.020	*	.052	*	.038	*
CR	.000	*	.000	*	.010	*	.008	*	.005	*	.000	*	.009	*	.016	*
FE	1.958	*	1.710	*	2.069	*	1.517	*	1.756	*	2.021	*	2.298	*	2.271	*
MG	2.897	*	3.232	*	2.664	*	3.502	*	2.819	*	2.609	*	2.254	*	2.273	*
MN	.048	5.028	.064	5.145	.037	5.085	.027	5.100	.039	4.974	.059	5.115	.042	5.217	.049	5.224
BA	.000	*	.000	*	.000	*	.000	*	.003	*	.006	*	.000	*	.003	*
CA	1.925	*	1.906	*	1.839	*	1.909	*	1.898	*	1.867	*	1.765	*	1.752	*
K	.065	*	.039	*	.124	*	.020	*	.052	*	.124	*	.034	*	.032	*
NA	.096	2.086	.101	2.045	.273	2.236	.022	1.951	.137	2.090	.254	2.251	.342	2.141	.319	2.107
F	.243	*	.000	*	.232	*	.000	*	.050	*	.014	*	.000	*	.000	*
CL	.000	*	.000	*	.000	*	.000	*	.000	*	.000	*	.000	*	.000	*
O	23.000	*	23.000	*	23.000	*	23.000	*	23.000	*	23.000	*	23.000	*	23.000	*
FE	40.33		34.60		43.71		30.22		38.38		43.65		50.48		49.97	
MG	59.67		65.40		56.29		69.78		61.62		56.35		49.52		50.03	
F/M	.692		.549		.791		.441		.637		.797		1.038		1.020	
F/FM	.409		.354		.442		.306		.389		.444		.509		.505	

9 MIN21-3 C2 - SPOT 2 - AMP BT
10 MIN21-3 C2 - SPOT 2 - AMP DK
11 MIN21-3 C2 - SPOT 8 - AMPH BT
12 MIN21-3 C2 - SPOT 8 - AMPH DK
13 MIN21-3 C2 - SPOT 9 - AMPH DK
14 MIN21-3 C2 - SPOT 9 - AMPH BT
15 *****MIN21-5 C1 - AMPH - SPOT 1
16 MIN21-5 C1 - AMPH - SPOT 2

AMPHIBOLE, RODERICK TOM-YING, KINGSBAY GOLD CORP., Feb 2012, R.G.C.

	17	18	19	20	21	22	23	24
SIO2	53.29	47.85	52.61	47.08	52.67	47.58	50.25	47.89
TIO2	.11	.51	.25	.38	.18	.49	.36	.28
A2O3	3.73	8.46	4.75	11.02	5.43	9.98	7.24	8.97
C2O3	.26	.24	.08	.16	.06	.03	.43	.26
FEO	16.60	18.38	16.31	17.93	15.61	17.69	15.81	16.22
MGO	13.22	10.43	13.13	9.16	12.67	9.60	11.31	10.71
MNO	.55	.42	.66	.33	.40	.28	.32	.34
K2O	.09	.15	.06	.23	.12	.18	.22	.19
CAO	10.19	11.03	9.80	11.34	10.64	11.16	11.38	11.49
NA2O	.43	1.21	.63	1.15	.68	1.31	.85	.98
BAO	.00	.00	.03	.00	.00	.00	.01	.32
F	.00	.03	.00	.00	.12	.00	.12	.43
CL	.00	.00	.00	.00	.00	.03	.00	.04
SUM	98.47	98.71	98.31	98.78	98.58	98.33	98.30	98.12
-O= F+CL	.00	.01	.00	.00	.05	.01	.05	.19
SUM	98.47	98.70	98.31	98.78	98.53	98.32	98.25	97.93

SI	7.704	*	7.050	*	7.609	*	6.908	*	7.577	*	7.002	*	7.312	*	7.042	*
AL	.296	8.000	.950	8.000	.391	8.000	1.092	8.000	.423	8.000	.998	8.000	.688	8.000	.958	8.000
AL	.339	*	.518	*	.419	*	.814	*	.497	*	.733	*	.554	*	.597	*
TI	.012	*	.057	*	.027	*	.042	*	.019	*	.054	*	.039	*	.031	*
CR	.030	*	.028	*	.009	*	.019	*	.007	*	.003	*	.049	*	.030	*
FE	2.007	*	2.265	*	1.973	*	2.200	*	1.878	*	2.177	*	1.924	*	1.995	*
MG	2.849	*	2.290	*	2.831	*	2.003	*	2.717	*	2.106	*	2.453	*	2.347	*
MN	.067	5.304	.052	5.210	.081	5.339	.041	5.119	.049	5.167	.035	5.108	.039	5.059	.042	5.042
BA	.000	*	.000	*	.002	*	.000	*	.000	*	.000	*	.001	*	.018	*
CA	1.578	*	1.741	*	1.519	*	1.783	*	1.640	*	1.760	*	1.774	*	1.810	*
K	.017	*	.028	*	.011	*	.043	*	.022	*	.034	*	.041	*	.036	*
NA	.121	1.715	.346	2.115	.177	1.708	.327	2.153	.190	1.852	.374	2.167	.240	2.056	.279	2.144
F	.000	*	.014	*	.000	*	.000	*	.055	*	.000	*	.055	*	.200	*
CL	.000	*	.000	*	.000	*	.000	*	.000	*	.007	*	.000	*	.010	*
O	23.000	*	23.000	*	23.000	*	23.000	*	23.000	*	23.000	*	23.000	*	23.000	*
FE	41.33		49.72		41.07		52.34		40.87		50.83		43.96		45.94	
MG	58.67		50.28		58.93		47.66		59.13		49.17		56.04		54.06	
F/M	.728		1.012		.726		1.119		.709		1.050		.800		.868	
F/FM	.421		.503		.420		.528		.415		.512		.445		.465	

17 MIN21-5 C1 - AMPH - SPOT 3 - DK DOMAIN
18 MIN21-5 C1 - AMPH - SPOT 3 - BT DOMAIN
19 MIN21-5 C1 - AMPH - SPOT 4 - DK DOMAIN
20 MIN21-5 C1 - AMPH - SPOT 4 - BT DOMAIN
21 MIN21-5 C1 - AMPH - SPOT 5 - DK DOMAIN
22 MIN21-5 C1 - AMPH - SPOT 5 - BT DOMAIN
23 MIN21-5 C1 - AMPH - SPOT 6 - DK DOMAIN
24 MIN21-5 C1 - AMPH - SPOT 6 - BT DOMAIN

AMPHIBOLE, RODERICK TOM-YING, KINGSBAY GOLD CORP., Feb 2012, R.G.C.

	25	26	27	28	29	30	31	32
SIO2	48.22	50.63	46.84	50.15	50.57	47.31	50.22	53.34
TIO2	.45	.20	.77	.59	.51	.82	.47	.00
A2O3	8.49	6.07	8.43	5.70	5.71	7.01	5.10	1.66
C2O3	.10	.08	.00	.05	.07	.10	.11	.11
FEO	17.51	16.77	19.61	19.40	17.26	19.05	17.15	14.78
MGO	10.24	11.43	9.23	9.52	11.15	10.14	11.84	14.17
MNO	.28	.57	.63	.58	.67	.65	.73	.81
K2O	.15	.13	.25	.17	.12	.21	.13	.06
CAO	11.07	11.68	11.48	11.57	11.65	11.53	11.76	12.69
NA2O	1.29	.72	1.21	.82	.80	1.15	.81	.11
BAO	.00	.13	.04	.00	.13	.00	.08	.05
F	.00	.00	.04	.00	.00	.61	.06	.53
CL	.00	.00	.02	.00	.02	.01	.00	.01
SUM	97.80	98.41	98.55	98.55	98.66	98.59	98.46	98.32
-O= F+CL	.00	.00	.02	.00	.00	.26	.03	.23
SUM	97.80	98.41	98.53	98.55	98.66	98.33	98.43	98.09

SI	7.128	*	7.404	*	6.988	*	7.416	*	7.403	*	7.041	*	7.381	*	7.739	*
AL	.872	8.000	.596	8.000	1.012	8.000	.584	8.000	.597	8.000	.959	8.000	.619	8.000	.261	8.000
AL	.607	*	.450	*	.470	*	.410	*	.388	*	.271	*	.264	*	.023	*
TI	.050	*	.022	*	.086	*	.066	*	.056	*	.092	*	.052	*	.000	*
CR	.012	*	.009	*	.000	*	.006	*	.008	*	.012	*	.013	*	.013	*
FE	2.165	*	2.051	*	2.447	*	2.399	*	2.113	*	2.371	*	2.108	*	1.793	*
MG	2.256	*	2.491	*	2.053	*	2.098	*	2.433	*	2.249	*	2.594	*	3.064	*
MN	.035	5.124	.071	5.094	.080	5.135	.073	5.051	.083	5.082	.082	5.077	.091	5.121	.100	4.993
BA	.000	*	.007	*	.002	*	.000	*	.007	*	.000	*	.005	*	.003	*
CA	1.753	*	1.830	*	1.835	*	1.833	*	1.827	*	1.839	*	1.852	*	1.973	*
K	.028	*	.024	*	.048	*	.032	*	.022	*	.040	*	.024	*	.011	*
NA	.370	2.151	.204	2.066	.350	2.235	.235	2.100	.227	2.084	.332	2.210	.231	2.112	.031	2.018
F	.000	*	.000	*	.019	*	.000	*	.000	*	.287	*	.028	*	.243	*
CL	.000	*	.000	*	.005	*	.000	*	.005	*	.003	*	.000	*	.002	*
O	23.000	*	23.000	*	23.000	*	23.000	*	23.000	*	23.000	*	23.000	*	23.000	*
FE	48.96		45.15		54.38		53.34		46.48		51.32		44.83		36.92	
MG	51.04		54.85		45.62		46.66		53.52		48.68		55.17		63.08	
F/M	.975		.852		1.231		1.178		.903		1.091		.848		.618	
F/FM	.494		.460		.552		.541		.474		.522		.459		.382	

25 MIN21-5 C1 - AMP - SPOT 12
26 *****GAL 5 - C1 - HB - SPOT 1 - DK DOMAIN
27 GAL 5 - C1 - HB - SPOT 1 - BT DOMAIN
28 GAL 5 - C1 - HB - SPOT 2 - MAIN GRAIN
29 GAL 5 - C1 - HB - SPOT 3 - DK DOMAIN CORE
30 GAL 5 - C1 - HB - SPOT 3 - BT DOMAIN MARGINAL
31 GAL 5 - C1 - HB - SPOT 8 - MAIN GRAIN
32 GAL 5 - C2 - HB - SPOT 1 - DK DOMAIN

AMPHIBOLE, RODERICK TOM-YING, KINGSBAY GOLD CORP., Feb 2012, R.G.C.

	33	34	35	36	37	38	39	40
SIO2	50.06	53.21	50.33	53.80	49.69	53.88	49.49	55.45
TIO2	.42	.00	.41	.02	.57	.03	.10	.00
A2O3	5.03	3.40	4.59	2.86	5.50	1.06	8.16	.76
C2O3	.20	.01	.09	.03	.13	.02	.00	.00
FEO	17.86	14.37	17.55	14.74	17.68	13.80	17.16	13.39
MGO	11.63	12.97	11.96	13.07	11.68	15.17	9.36	15.56
MNO	.60	.68	.77	.57	.65	.83	.69	.88
K2O	.13	.07	.12	.03	.13	.04	.26	.03
CAO	11.73	13.45	11.84	13.11	11.66	12.92	11.99	12.62
NA2O	.69	.11	.73	.12	.77	.05	1.00	.02
BAO	.00	.00	.00	.11	.11	.16	.00	.00
F	.00	.00	.73	.00	.00	.47	.00	.00
CL	.01	.02	.01	.00	.00	.01	.05	.02
SUM	98.36	98.29	99.13	98.46	98.57	98.44	98.26	98.73
-O= F+CL	.00	.00	.31	.00	.00	.20	.01	.00
SUM	98.36	98.29	98.82	98.46	98.57	98.24	98.25	98.73

SI	7.381	*	7.700	*	7.360	*	7.771	*	7.315	*	7.780	*	7.275	*	7.924	*
AL	.619	8.000	.300	8.000	.640	8.000	.229	8.000	.685	8.000	.180	7.960	.725	8.000	.076	8.000
AL	.255	*	.279	*	.151	*	.258	*	.270	*	.000	*	.688	*	.052	*
TI	.047	*	.000	*	.045	*	.002	*	.063	*	.003	*	.011	*	.000	*
CR	.023	*	.001	*	.010	*	.003	*	.015	*	.002	*	.000	*	.000	*
FE	2.202	*	1.739	*	2.146	*	1.780	*	2.177	*	1.666	*	2.109	*	1.600	*
MG	2.556	*	2.797	*	2.607	*	2.814	*	2.563	*	3.265	*	2.051	*	3.314	*
MN	.075	5.158	.083	4.900	.095	5.054	.070	4.927	.081	5.169	.102	5.038	.086	4.945	.107	5.072
BA	.000	*	.000	*	.000	*	.006	*	.006	*	.009	*	.000	*	.000	*
CA	1.853	*	2.085	*	1.855	*	2.029	*	1.839	*	1.999	*	1.888	*	1.932	*
K	.024	*	.013	*	.022	*	.006	*	.024	*	.007	*	.049	*	.005	*
NA	.197	2.075	.031	2.129	.207	2.084	.034	2.074	.220	2.090	.014	2.029	.285	2.222	.006	1.943
F	.000	*	.000	*	.338	*	.000	*	.000	*	.215	*	.000	*	.000	*
CL	.002	*	.005	*	.002	*	.000	*	.000	*	.002	*	.012	*	.005	*
O	23.000	*	23.000	*	23.000	*	23.000	*	23.000	*	23.000	*	23.000	*	23.000	*
FE	46.28		38.33		45.15		38.75		45.93		33.79		50.71		32.56	
MG	53.72		61.67		54.85		61.25		54.07		66.21		49.29		67.44	
F/M	.891		.651		.860		.658		.881		.541		1.071		.515	
F/FM	.471		.394		.462		.397		.468		.351		.517		.340	

33 GAL 5 - C2 - HB - SPOT 1 - BT DOMAIN
34 GAL 5 - C2 - HB - SPOT 2 - DK DOMAIN
35 GAL 5 - C2 - HB - SPOT 2 - BT DOMAIN
36 GAL 5 - C2 - HB - SPOT 3 - DK DOMAIN
37 GAL 5 - C2 - HB - SPOT 3 - BT DOMAIN
38 GAL 5 - C5 - AMP - SPOT 1 - DK DOMAIN
39 GAL 5 - C5 - AMP - SPOT 1 - BT DOMAIN
40 GAL 5 - C5 - AMP - SPOT 2 - DK DOMAIN

AMPHIBOLE, RODERICK TOM-YING, KINGSBAY GOLD CORP., Feb 2012, R.G.C.

	41	42	43	44
SIO2	51.08	54.89	49.93	55.63
TIO2	.05	.00	.21	.00
A2O3	4.24	.53	7.42	1.80
C2O3	.19	.01	.03	.00
FEO	16.85	13.90	16.45	9.67
MGO	12.33	15.19	9.76	17.05
MNO	.76	.73	.95	.76
K2O	.13	.02	.21	.04
CAO	12.37	12.97	12.48	13.01
NA2O	.45	.01	.81	.07
BAO	.14	.05	.11	.13
F	.00	.00	.00	.00
CL	.00	.01	.01	.01
SUM	98.59	98.31	98.37	98.17
-O= F+CL	.00	.00	.00	.00
SUM	98.59	98.31	98.37	98.17

SI	7.488	*	7.912	*	7.325	*	7.865	*
AL	.512	8.000	.088	8.000	.675	8.000	.135	8.000
AL	.220	*	.002	*	.607	*	.165	*
TI	.006	*	.000	*	.023	*	.000	*
CR	.022	*	.001	*	.003	*	.000	*
FE	2.066	*	1.676	*	2.018	*	1.143	*
MG	2.694	*	3.264	*	2.134	*	3.593	*
MN	.094	5.102	.089	5.032	.118	4.904	.091	4.992
BA	.008	*	.003	*	.006	*	.007	*
CA	1.943	*	2.003	*	1.962	*	1.971	*
K	.024	*	.004	*	.039	*	.007	*
NA	.128	2.103	.003	2.012	.230	2.238	.019	2.004
F	.000	*	.000	*	.000	*	.000	*
CL	.000	*	.002	*	.002	*	.002	*
O	23.000	*	23.000	*	23.000	*	23.000	*
	FE	43.40		33.92		48.60		24.14
	MG	56.60		66.08		51.40		75.86
	F/M	.802		.541		1.001		.344
	F/FM	.445		.351		.500		.256

41 GAL 5 - C5 - AMP - SPOT 2 - BT DOMAIN
42 GAL 5 - C5 - AMP - SPOT 3 - DK DOMAIN
43 GAL 5 - C5 - AMP - SPOT 3 - BT DOMAIN
44 GAL 5 - C3 - AMP - RELICT AMPH IN EPIDOTE SPOT 2

PLAGIOCLASE/FELDSPARS, RODERICK TOM-YING, KINGSBAY GOLD CORP., Feb 2012, R.G.C.

	1	2	3	4	5	6	7	8
SIO2	69.17	70.13	64.08	69.17	65.04	69.57	65.41	69.41
A2O3	18.43	17.19	17.41	18.76	18.08	18.92	17.94	20.14
K2O	.11	.05	15.83	.08	15.70	.06	15.59	.06
CAO	.20	.35	.00	.15	.00	.14	.02	.21
NA2O	11.90	11.63	.19	11.74	.32	11.54	.32	10.69
BAO	.00	.08	2.16	.01	1.00	.03	1.57	.08
SUM	99.81	99.43	99.67	99.91	100.14	100.26	100.85	100.59

SI	12.112	*	12.306	*	12.057	*	12.088	*	12.047	*	12.100	*	12.068	*	12.000	*
AL	3.803	15.915	3.554	15.860	3.860	15.917	3.863	15.952	3.946	15.993	3.878	15.978	3.900	15.969	4.000	16.000
AL	.000	*	.000	*	.000	*	.000	*	.000	*	.000	*	.000	*	.103	*
CA	.038	*	.066	*	.000	*	.028	*	.000	*	.026	*	.004	*	.039	*
NA	4.040	*	3.957	*	.069	*	3.978	*	.115	*	3.892	*	.114	*	3.583	*
K	.025	*	.011	*	3.799	*	.018	*	3.709	*	.013	*	3.669	*	.013	*
BA	.000	4.102	.006	4.039	.159	4.027	.001	4.024	.073	3.896	.002	3.933	.114	3.901	.005	3.744
O	32.000	*	32.000	*	32.000	*	32.000	*	32.000	*	32.000	*	32.000	*	32.000	*
	ALBI	98.49		98.09		1.79		98.86		3.01		99.00		3.02		98.57
	ORTH	.60		.28		98.21		.44		96.99		.34		96.87		.36
	ANOR	.91		1.63		.00		.70		.00		.66		.10		1.07

1 *****GAL 9 - C3 - ALBITE - SPOT 3
2 GAL 9 - C3 - ALBITE - SPOT 3
3 GAL 9 - C1 - KSPAR BT DOMAIN - SPOT 1
4 GAL 9 - C1 - ALBITE - SPOT 2
5 GAL 9 - C2 - KSPAR - SPOT 1
6 GAL 9 - C2 - ALBITE - SPOT 4
7 GAL 9 - C2 - KSPAR - SPOT 2
8 GAL 9 - C6 - ALBITE - SPOT 2

PLAGIOCLASE/FELDSPARS, RODERICK TOM-YING, KINGSBAY GOLD CORP., Feb 2012, R.G.C.

	9	10	11	12	13	14	15	16
SIO2	58.86	59.75	59.52	59.88	59.36	61.41	63.63	59.90
A2O3	25.97	25.04	25.68	24.84	24.75	24.68	22.26	24.49
K2O	.05	.06	.08	.05	.08	.12	.08	.10
CAO	8.96	8.37	8.26	8.38	8.93	7.15	4.25	7.93
NA2O	6.37	6.99	7.08	7.16	6.56	7.29	8.95	6.94
BAO	.16	.01	.00	.06	.00	.08	.00	.00
SUM	100.37	100.22	100.62	100.37	99.68	100.73	99.17	99.36
SI	10.493 *	10.648 *	10.569 *	10.666 *	10.644 *	10.839 *	11.318 *	10.745 *
AL	5.455 15.948	5.258 15.907	5.373 15.942	5.214 15.879	5.230 15.874	5.133 15.973	4.666 15.984	5.177 15.922
AL	.000 *	.000 *	.000 *	.000 *	.000 *	.000 *	.000 *	.000 *
CA	1.711 *	1.598 *	1.571 *	1.599 *	1.716 *	1.352 *	.810 *	1.524 *
NA	2.202 *	2.415 *	2.437 *	2.473 *	2.281 *	2.495 *	3.087 *	2.414 *
K	.011 *	.014 *	.018 *	.011 *	.018 *	.027 *	.018 *	.023 *
BA	.011 3.935	.001 4.028	.000 4.027	.004 4.087	.000 4.015	.006 3.879	.000 3.915	.000 3.961
O	32.000 *	32.000 *	32.000 *	32.000 *	32.000 *	32.000 *	32.000 *	32.000 *
	ALBI 56.10	59.98	60.53	60.56	56.81	64.40	78.85	60.94
	ORTH .29	.34	.45	.28	.46	.70	.46	.58
	ANOR 43.61	39.69	39.02	39.17	42.74	34.90	20.69	38.48

9 *****MIN21-5 C1 - PLAG - SPOT 7
10 MIN21-5 C1 - PLAG - SPOT 8
11 MIN21-5 C1 - PLAG - SPOT 9
12 MIN21-5 C1 - PLAG - SPOT 10
13 MIN21-5 C1 - PLAG - SPOT 11
14 *****GAL 6 - C1 - KSPAR - SPOT 1 - CORE
15 GAL 6 - C1 - PLAG - SPOT 2 - DK BAND
16 GAL 6 - C1 - PLAG - SPOT 3 - BT BAND

PLAGIOCLASE/FELDSPARS, RODERICK TOM-YING, KINGSBAY GOLD CORP., Feb 2012, R.G.C.

	17	18	19	20	21	22	23	24
SIO2	61.48	60.74	59.80	64.80	64.32	60.06	61.43	60.64
A2O3	24.49	24.88	24.51	21.71	22.05	25.17	24.75	23.76
K2O	.10	.10	.09	.09	.08	.10	.10	.10
CAO	6.29	7.97	7.80	4.61	4.23	8.15	6.87	7.41
NA2O	7.77	6.99	7.71	8.89	9.42	6.50	7.19	7.50
BAO	.00	.03	.00	.11	.13	.06	.00	.06
SUM	100.13	100.71	99.91	100.21	100.23	100.04	100.34	99.47
SI	10.894 *	10.747 *	10.701 *	11.416 *	11.347 *	10.692 *	10.860 *	10.866 *
AL	5.106 16.000	5.187 15.934	5.168 15.869	4.507 15.923	4.584 15.931	5.280 15.973	5.140 16.000	5.017 15.882
AL	.007 *	.000 *	.000 *	.000 *	.000 *	.000 *	.015 *	.000 *
CA	1.194 *	1.511 *	1.495 *	.870 *	.800 *	1.555 *	1.301 *	1.423 *
NA	2.669 *	2.398 *	2.675 *	3.036 *	3.222 *	2.244 *	2.464 *	2.606 *
K	.023 *	.023 *	.021 *	.020 *	.018 *	.023 *	.023 *	.023 *
BA	.000 3.893	.002 3.933	.000 4.191	.008 3.934	.009 4.048	.004 3.825	.000 3.803	.004 4.055
O	32.000 *	32.000 *	32.000 *	32.000 *	32.000 *	32.000 *	32.000 *	32.000 *
ALBI	68.69	60.99	63.83	77.33	79.76	58.72	65.05	64.32
ORTH	.58	.57	.49	.51	.45	.59	.60	.56
ANOR	30.73	38.43	35.68	22.16	19.79	40.69	34.35	35.12

17 GAL 6 - C1 - PLAG - SPOT 4 - DK BAND
18 GAL 6 - C1 - PLAG - SPOT 5 - BT BAND
19 GAL 6 - C1 - PLAG - SPOT 6 - DK BAND
20 GAL 6 - C1 - PLAG - SPOT 7 - OUTER MARGIN
21 GAL 6 - C2 - PLAG - SPOT 1 - CORE
22 GAL 6 - C2 - PLAG - SPOT 2 - BT BAND
23 GAL 6 - C2 - PLAG - SPOT 3 - DK BAND
24 GAL 6 - C2 - PLAG - SPOT 4 - BT BAND

PLAGIOCLASE/FELDSPARS, RODERICK TOM-YING, KINGSBAY GOLD CORP., Feb 2012, R.G.C.

	25	26	27	28	29	30	31	32
SIO2	60.85	60.49	61.10	64.47	63.94	64.19	61.40	64.42
A2O3	23.74	24.02	24.03	22.02	22.45	22.31	24.26	22.03
K2O	.11	.12	.09	.11	.07	.12	.09	.07
CAO	6.76	7.30	7.23	4.51	5.09	4.65	7.16	4.53
NA2O	7.86	7.52	7.48	9.16	8.33	8.45	7.12	8.91
BAO	.10	.06	.00	.06	.18	.05	.06	.00
SUM	99.42	99.51	99.93	100.33	100.06	99.77	100.09	99.96
SI	10.900 *	10.834 *	10.878 *	11.355 *	11.291 *	11.342 *	10.894 *	11.369 *
AL	5.011 15.911	5.070 15.904	5.041 15.919	4.570 15.926	4.671 15.962	4.645 15.988	5.072 15.967	4.581 15.950
AL	.000 *	.000 *	.000 *	.000 *	.000 *	.000 *	.000 *	.000 *
CA	1.297 *	1.401 *	1.379 *	.851 *	.963 *	.880 *	1.361 *	.857 *
NA	2.730 *	2.611 *	2.582 *	3.128 *	2.852 *	2.895 *	2.449 *	3.049 *
K	.025 *	.027 *	.020 *	.025 *	.016 *	.027 *	.020 *	.016 *
BA	.007 4.059	.004 4.044	.000 3.981	.004 4.008	.012 3.843	.003 3.806	.004 3.835	.000 3.921
O	32.000 *	32.000 *	32.000 *	32.000 *	32.000 *	32.000 *	32.000 *	32.000 *
	ALBI 67.36	64.64	64.85	78.13	74.45	76.14	63.94	77.75
	ORTH .62	.68	.51	.62	.41	.71	.53	.40
	ANOR 32.02	34.68	34.64	21.26	25.14	23.15	35.53	21.85

25 GAL 6 - C2 - PLAG - SPOT 5 - DK BAND
26 GAL 6 - C2 - PLAG - SPOT 6 - BT BAND
27 GAL 6 - C2 - PLAG - SPOT 7 - BT BAND
28 GAL 6 - C2 - PLAG - SPOT 8 - MARGIN
29 GAL 6 - C3 - PLAG - SPOT 1 - CORE
30 GAL 6 - C3 - PLAG - SPOT 2 - MARGIN
31 GAL 6 - C3 - PLAG - SPOT 3 - MID
32 GAL 6 - C3 - PLAG - SPOT 4

PLAGIOCLASE/FELDSPARS, RODERICK TOM-YING, KINGSBAY GOLD CORP., Feb 2012, R.G.C.

	33	34	35	36	37	38	39	40
SIO2	62.65	60.53	60.52	61.20	60.99	60.46	62.32	62.53
A2O3	23.46	24.32	25.38	24.87	24.57	25.06	23.50	23.56
K2O	.10	.11	.11	.11	.09	.09	.13	.10
CAO	5.35	6.56	6.65	6.86	6.81	7.87	6.33	5.49
NA2O	8.66	7.71	7.59	7.55	7.64	7.05	7.86	8.79
BAO	.00	.00	.00	.11	.01	.00	.00	.06
SUM	100.22	99.23	100.25	100.70	100.11	100.53	100.14	100.53
SI	11.078 *	10.843 *	10.731 *	10.811 *	10.831 *	10.715 *	11.038 *	11.042 *
AL	4.888 15.966	5.134 15.977	5.269 16.000	5.177 15.987	5.142 15.973	5.234 15.949	4.905 15.942	4.903 15.945
AL	.000 *	.000 *	.034 *	.000 *	.000 *	.000 *	.000 *	.000 *
CA	1.014 *	1.259 *	1.263 *	1.298 *	1.296 *	1.494 *	1.201 *	1.039 *
NA	2.969 *	2.678 *	2.609 *	2.586 *	2.631 *	2.423 *	2.699 *	3.010 *
K	.023 *	.025 *	.025 *	.025 *	.020 *	.020 *	.029 *	.023 *
BA	.000 4.005	.000 3.962	.000 3.932	.008 3.916	.001 3.947	.000 3.937	.000 3.930	.004 4.075
O	32.000 *	32.000 *	32.000 *	32.000 *	32.000 *	32.000 *	32.000 *	32.000 *
ALBI	74.13	67.59	66.95	66.15	66.65	61.53	68.68	73.93
ORTH	.56	.63	.64	.63	.52	.52	.75	.55
ANOR	25.31	31.78	32.41	33.22	32.83	37.96	30.57	25.52

33 GAL 6 - C4 - PLAG - SPOT 2
34 GAL 6 - C5 - PLAG - SPOT 1
35 GAL 6 - C5 - PLAG - SPOT 2 DK
36 GAL 6 - C5 - PLAG - SPOT 3 BT
37 GAL 6 - C5 - PLAG - SPOT 4 DK
38 GAL 6 - C5 - PLAG - SPOT 5 BT
39 GAL 6 - C5 - PLAG - SPOT 6 BT
40 GAL 6 - C5 - PLAG - SPOT 7 MARGIN

PLAGIOCLASE/FELDSPARS, RODERICK TOM-YING, KINGSBAY GOLD CORP., Feb 2012, R.G.C.

	41	42	43	44	45	46
SIO2	61.99	63.66	64.38	63.08	64.40	64.60
A2O3	24.35	23.87	21.34	23.25	21.50	21.35
K2O	.08	.12	.09	.07	.07	.11
CAO	5.96	5.01	4.38	5.66	4.56	5.46
NA2O	8.16	8.14	10.04	8.42	9.09	8.58
BAO	.18	.13	.06	.45	.06	.06
SUM	100.72	100.93	100.29	100.93	99.68	100.16

SI	10.932	*	11.137	*	11.382	*	11.108	*	11.412	*	11.408	*
AL	5.060	15.992	4.863	16.000	4.446	15.828	4.825	15.933	4.490	15.902	4.443	15.850
AL	.000	*	.058	*	.000	*	.000	*	.000	*	.000	*
CA	1.126	*	.939	*	.830	*	1.068	*	.866	*	1.033	*
NA	2.790	*	2.761	*	3.441	*	2.875	*	3.123	*	2.938	*
K	.018	*	.027	*	.020	*	.016	*	.016	*	.025	*
BA	.012	3.947	.009	3.794	.004	4.296	.031	3.989	.004	4.009	.004	4.000
O	32.000	*	32.000	*	32.000	*	32.000	*	32.000	*	32.000	*
	ALBI	70.92		74.08		80.19		72.62		77.99		73.52
	ORTH	.46		.72		.47		.40		.40		.62
	ANOR	28.62		25.20		19.33		26.98		21.62		25.86

41 *****GAL 5 - C1 - PLAG - SPOT 4
42 GAL 5 - C1 - PLAG - SPOT 5
43 GAL 5 - C1 - PLAG - SPOT 6
44 GAL 5 - C1 - PLAG - SPOT 7
45 GAL 5 - C2 - PLAG - SPOT 4
46 GAL 5 - C2 - PLAG - SPOT 5

PYROXENE, RODERICK TOM-YING, KINGSBAY GOLD CORP., Feb 2012 R.G.C.

	1	2	3	4	5	6	7
SIO2	52.70	51.77	50.62	52.01	51.76	51.54	51.13
TIO2	.00	.00	.10	.14	.00	.08	.01
A2O3	.62	.48	.43	1.32	.78	.58	.49
C2O3	.00	.10	.03	.00	.02	.00	.04
FEO	13.25	14.20	15.24	13.01	13.21	13.97	16.27
MGO	9.65	9.38	9.16	10.05	9.94	9.75	8.36
MNO	.60	.81	.72	.37	.50	.71	.93
K2O	.00	.01	.03	.03	.01	.02	.02
CAO	23.31	22.82	23.45	23.33	23.55	23.42	23.43
NA2O	.27	.30	.21	.38	.34	.21	.17
SUM	100.40	99.87	99.99	100.64	100.11	100.28	100.85

SI	2.005	*	1.994	*	1.965	*	1.974	*	1.981	*	1.978	*	1.975	*
AL	.000	2.005	.006	2.000	.020	1.985	.026	2.000	.019	2.000	.022	2.000	.022	1.997
AL	.028	*	.016	*	.000	*	.033	*	.016	*	.004	*	.000	*
TI	.000	*	.000	*	.003	*	.004	*	.000	*	.002	*	.000	*
CR	.000	*	.003	*	.001	*	.000	*	.001	*	.000	*	.001	*
FE	.422	*	.457	*	.495	*	.413	*	.423	*	.448	*	.526	*
MN	.019	*	.026	*	.024	*	.012	*	.016	*	.023	*	.030	*
MG	.547	*	.538	*	.530	*	.568	*	.567	*	.558	*	.481	*
CA	.950	*	.942	*	.975	*	.948	*	.966	*	.963	*	.970	*
K	.000	*	.000	*	.001	*	.001	*	.000	*	.001	*	.001	*
NA	.020	*	.022	*	.016	*	.028	*	.025	*	.016	*	.013	*
COMP	.000	1.986	.000	2.005	.000	2.045	2.000	2.008	.000	2.014	6.000	2.015	.000	2.022
O	.000	*	.000	*	.000	*	.000	*	.000	*	.000	*	.000	*
ENST	28.52		27.79		26.50		29.46		29.00		28.32		24.35	
FERR	21.97		23.61		24.74		21.39		21.62		22.77		26.59	
WOLL	49.51		48.60		48.76		49.15		49.38		48.91		49.06	
F/M	.806		.898		.978		.747		.774		.845		1.155	
F/FM	.446		.473		.494		.428		.436		.458		.536	

1 *****GAL 5 - C3 - CPX - SPOT 4
2 GAL 5 - C3 - CPX - SPOT 5
3 GAL 5 - C3 - CPX - RANDOM ZONED BT OUTER
4 GAL 5 - C3 - CPX - RANDOM ZONED DK
5 GAL 5 - C3 - CPX - RANDOM ZONED INT
6 GAL 5 - C3 - CPX - ANOTHER ZONED DK
7 GAL 5 - C3 - CPX - ANOTHER ZONED BT

EPIDOTE, RODERICK TOM-YING, KINGSBAY GOLD CORP., Feb 2012, R.G.C.

	1	2	3	4	5	6	7	8
SIO2	39.28	38.19	38.43	38.05	38.48	39.91	42.39	38.90
TIO2	.07	.06	.17	.30	.11	.05	.10	.02
A2O3	23.77	23.62	23.12	24.62	23.08	27.06	26.12	29.06
C2O3	.06	.07	.06	.07	.00	.07	.00	.00
FEO	12.40	13.95	14.02	12.56	13.83	8.63	8.43	6.54
MGO	.03	.02	.07	.03	.00	.00	.00	.01
MNO	.07	.22	.15	.04	.16	.08	.10	.28
K2O	.01	.03	.02	.02	.01	.02	.02	.01
CAO	23.20	23.36	22.72	23.05	23.16	23.60	21.51	23.32
NA2O	.00	.00	.00	.02	.00	.02	.01	.02
SUM	98.89	99.52	98.76	98.76	98.83	99.44	98.68	98.16

SI	3.271	*	3.198	*	3.236	*	3.181	*	3.239	*	3.234	*	3.416	*	3.162	*
AL	.000	3.271	.000	3.198	.000	3.236	.000	3.181	.000	3.239	.000	3.234	.000	3.416	.000	3.162
AL	2.333	*	2.331	*	2.294	*	2.426	*	2.289	*	2.584	*	2.480	*	2.783	*
TI	.004	*	.004	*	.011	*	.019	*	.007	*	.003	*	.006	*	.001	*
CR	.004	*	.005	*	.004	*	.005	*	.000	*	.004	*	.000	*	.000	*
FE	.864	*	.977	*	.987	*	.878	*	.973	*	.585	*	.568	*	.445	*
MN	.005	*	.016	*	.011	*	.003	*	.011	*	.005	*	.007	*	.019	*
MG	.004	*	.002	*	.009	*	.004	*	.000	*	.000	*	.000	*	.001	*
CA	2.070	*	2.096	*	2.050	*	2.065	*	2.088	*	2.049	*	1.857	*	2.031	*
K	.001	*	.003	*	.002	*	.002	*	.001	*	.002	*	.002	*	.001	*
NA	.000	5.284	.000	5.433	.000	5.368	.003	5.404	.000	5.370	.003	5.236	.002	4.922	.003	5.284
O	13.000	*	13.000	*	13.000	*	13.000	*	13.000	*	13.000	*	13.000	*	13.000	*
	F/M	233.237		397.601		113.593		235.661		.000		.000		.000		382.855
	F/FM	.996		.997		.991		.996		.000		.000		.000		.997

1 *****MIN21-3 C2 - SPOT 10 - EPIDOTE
2 MIN21-3 C2 - SPOT 11 - EPIDOTE
3 MIN21-3 C2 - SPOT 12 - EPIDOTE BT
4 MIN21-3 C2 - SPOT 12 - EPIDOTE DK
5 MIN21-3 C2 - RANDOM EPIDOTE
6 *****GAL 5 - C1 - EP - SPOT 8 - DK ZONE
7 GAL 5 - C2 - EP - SPOT 6
8 GAL 5 - C3 - EP - SPOT 1

	9		10	
SIO2	38.87		39.51	
TIO2	.07		.02	
A2O3	27.63		25.52	
C2O3	.00		.03	
FEO	8.02		9.74	
MGO	.02		.02	
MNO	.09		.26	
K2O	.01		.03	
CAO	23.36		23.39	
NA2O	.01		.21	
SUM	98.08		98.73	
SI	3.187	*	3.253	*
AL	.000	3.187	.000	3.253
AL	2.669	*	2.476	*
TI	.004	*	.001	*
CR	.000	*	.002	*
FE	.550	*	.671	*
MN	.006	*	.018	*
MG	.002	*	.002	*
CA	2.052	*	2.063	*
K	.001	*	.003	*
NA	.002	5.287	.034	5.271
O	13.000	*	13.000	*
F/M	227.548		280.631	
F/FM	.996		.996	

9 GAL 5 - C3 - EP - SPOT 3
10 GAL 5 - C1 - EP - SPOT 2 - DK CENTRAL

MICA, RODERICK TOM YING, KINGSBAY GOLD CORP., Feb 2012, R.G.C.

	1	2	3	4	5	6	7	8
SIO2	46.29	46.71	46.82	47.18	47.29	47.48	46.93	47.63
TIO2	.59	.45	.26	.18	.18	.24	.31	.27
A2O3	30.74	30.07	31.19	30.49	31.39	30.72	31.96	31.74
C2O3	.05	.08	.00	.00	.00	.08	.00	.00
FEO	5.27	5.07	4.67	5.44	5.11	4.91	4.08	5.09
MGO	1.12	1.09	1.12	1.10	1.09	1.03	.90	1.07
MNO	.06	.02	.00	.11	.07	.00	.02	.05
K2O	11.48	12.06	11.87	10.94	10.95	10.63	10.61	9.51
CAO	.00	.00	.00	.00	.00	.01	.00	.00
NA2O	.09	.11	.12	.06	.11	.01	.16	.12
BAO	.23	.30	.47	.18	.28	.63	.68	.80
F	.00	.17	.00	.00	.00	.09	.01	.08
CL	.00	.00	.01	.00	.02	.01	.01	.02
SUM	95.92	96.13	96.53	95.68	96.49	95.84	95.67	96.38
-O= F+CL	.00	.07	.00	.00	.00	.04	.01	.04
SUM	95.92	96.06	96.53	95.68	96.49	95.80	95.66	96.34

SI	6.305	*	6.366	*	6.333	*	6.410	*	6.362	*	6.425	*	6.341	*	6.377	*
AL	1.695	8.000	1.634	8.000	1.667	8.000	1.590	8.000	1.638	8.000	1.575	8.000	1.659	8.000	1.623	8.000
AL	3.239	*	3.195	*	3.305	*	3.291	*	3.338	*	3.324	*	3.429	*	3.384	*
TI	.060	*	.046	*	.026	*	.018	*	.018	*	.024	*	.031	*	.027	*
CR	.005	*	.009	*	.000	*	.000	*	.000	*	.009	*	.000	*	.000	*
FE	.600	*	.578	*	.528	*	.618	*	.575	*	.556	*	.461	*	.570	*
MG	.227	*	.221	*	.226	*	.223	*	.219	*	.208	*	.181	*	.214	*
MN	.007	4.140	.002	4.051	.000	4.085	.013	4.163	.008	4.158	.000	4.120	.002	4.106	.006	4.200
CA	.000	*	.000	*	.000	*	.000	*	.000	*	.001	*	.000	*	.000	*
BA	.012	*	.016	*	.025	*	.010	*	.015	*	.033	*	.036	*	.042	*
K	1.994	*	2.096	*	2.048	*	1.896	*	1.879	*	1.835	*	1.828	*	1.624	*
NA	.024	2.031	.029	2.141	.031	2.104	.016	1.921	.029	1.922	.003	1.872	.042	1.906	.031	1.697
F	.000	*	.073	*	.000	*	.000	*	.000	*	.039	*	.004	*	.034	*
CL	.000	*	.000	*	.002	*	.000	*	.005	*	.002	*	.002	*	.005	*
O	22.000	*	22.000	*	22.000	*	22.000	*	22.000	*	22.000	*	22.000	*	22.000	*
FE	72.53		72.30		70.06		73.51		72.45		72.79		71.78		72.74	
MG	27.47		27.70		29.94		26.49		27.55		27.21		28.22		27.26	
F/M	2.671		2.620		2.339		2.832		2.667		2.675		2.556		2.696	
F/FM	.728		.724		.701		.739		.727		.728		.719		.729	

1 ****GAL 9 - C3 - WHITE MICA - SPOT 1
2 GAL 9 - C3 - WHITE MICA - BT DOMAIN
3 GAL 9 - C3 - WHITE MICA - SPOT 2
4 GAL 9 - C2 - MICA - SPOT 3
5 GAL 9 - ANOTHER SPOT
6 GAL 9 - C4 - MICA - SPOT 1
7 GAL 9 - C4 - MICA - SPOT 2
8 GAL 9 - C4 - MICA - SPOT 3

MICA, RODERICK TOM YING, KINGSBAY GOLD CORP., Feb 2012, R.G.C.

	9	10	11	12	13	14	15	16
SIO2	46.05	37.78	37.20	37.17	37.19	37.34	37.75	47.66
TIO2	.29	.82	.89	1.02	.94	.89	.82	.00
A2O3	34.34	16.76	15.88	16.33	16.64	15.39	15.87	32.58
C2O3	.00	.12	.04	.04	.07	.06	.09	.00
FEO	4.49	18.12	20.38	19.59	19.30	19.79	19.95	2.92
MGO	.42	12.70	12.96	12.81	12.57	12.47	12.33	1.91
MNO	.03	.16	.22	.40	.33	.28	.18	.03
K2O	9.97	9.50	8.61	8.46	9.14	9.45	9.22	9.52
CAO	.00	.02	.05	.00	.00	.00	.05	.00
NA2O	.17	.03	.05	.05	.07	.02	.05	.14
BAO	.00	.00	.40	.17	.30	.35	.00	1.45
F	.64	.00	.21	.10	.08	.05	.02	.06
CL	.00	.00	.00	.01	.00	.02	.02	.02
SUM	96.40	96.01	96.89	96.15	96.63	96.11	96.35	96.29
-O= F+CL	.27	.00	.09	.04	.03	.03	.01	.03
SUM	96.13	96.01	96.80	96.11	96.60	96.08	96.34	96.26

SI	6.133	*	5.658	*	5.586	*	5.590	*	5.581	*	5.667	*	5.683	*	6.350	*
AL	1.867	8.000	2.342	8.000	2.414	8.000	2.410	8.000	2.419	8.000	2.333	8.000	2.317	8.000	1.650	8.000
AL	3.521	*	.616	*	.397	*	.484	*	.524	*	.419	*	.498	*	3.464	*
TI	.029	*	.092	*	.101	*	.115	*	.106	*	.102	*	.093	*	.000	*
CR	.000	*	.014	*	.005	*	.005	*	.008	*	.007	*	.011	*	.000	*
FE	.500	*	2.269	*	2.559	*	2.464	*	2.422	*	2.512	*	2.511	*	.325	*
MG	.083	*	2.835	*	2.901	*	2.871	*	2.812	*	2.821	*	2.766	*	.379	*
MN	.003	4.137	.020	5.847	.028	5.990	.051	5.990	.042	5.914	.036	5.897	.023	5.902	.003	4.172
CA	.000	*	.003	*	.008	*	.000	*	.000	*	.000	*	.008	*	.000	*
BA	.000	*	.000	*	.024	*	.010	*	.018	*	.021	*	.000	*	.076	*
K	1.693	*	1.815	*	1.649	*	1.623	*	1.749	*	1.829	*	1.770	*	1.618	*
NA	.044	1.737	.009	1.827	.015	1.695	.015	1.647	.020	1.787	.006	1.856	.015	1.793	.036	1.730
F	.270	*	.000	*	.100	*	.048	*	.038	*	.024	*	.010	*	.025	*
CL	.000	*	.000	*	.000	*	.003	*	.000	*	.005	*	.005	*	.005	*
O	22.000	*	22.000	*	22.000	*	22.000	*	22.000	*	22.000	*	22.000	*	22.000	*
	FE	85.71		44.46		46.87		46.18		46.28		47.10		47.58		46.17
	MG	14.29		55.54		53.13		53.82		53.72		52.90		52.42		53.83
	F/M	6.039		.808		.892		.876		.876		.903		.916		.867
	F/FM	.858		.447		.471		.467		.467		.475		.478		.464

9 GAL 9 - C6 - MICA IN FELD - SPOT 1
10 *****MIN21-3 C2 - SPOT 1 - BIOTITE
11 MIN21-3 C2 - SPOT 3 - BT
12 MIN21-3 C2 - SPOT 4 - BT
13 MIN21-3 C2 - SPOT 5 - BT
14 MIN21-3 C2 - SPOT 6 - BT
15 MIN21-3 C2 - SPOT 7 - BT
16 *****GAL 6 - C3 - MICA - SPOT 5

GARNET, RODERICK TOM-YING, KINGSBAY GOLD CORP., Feb 2012, R.G.C.

	1	2	3	4	5	6	7	8
SIO2	37.64	38.54	39.01	38.02	38.49	38.48	38.49	38.94
TIO2	.28	.21	.35	.52	.20	.36	.19	.44
A2O3	20.04	16.76	17.92	16.94	19.24	19.47	17.39	17.72
C2O3	.01	.02	.04	.06	.01	.00	.00	.01
FEO	5.17	9.14	7.31	8.76	5.37	5.58	9.45	8.99
MGO	.04	.06	.09	.05	.12	.08	.07	.08
MNO	1.24	3.15	1.99	1.87	.89	1.38	3.46	1.81
CAO	35.69	32.45	33.52	33.92	36.29	34.94	31.88	32.17
NA2O	.00	.00	.01	.01	.00	.00	.00	.00
SUM	100.11	100.33	100.23	100.14	100.61	100.29	100.93	100.16

SI	5.835	*	6.076	*	6.074	*	5.996	*	5.936	*	5.946	*	6.033	*	6.087	*
AL	.165	6.000	.000	6.076	.000	6.074	.004	6.000	.064	6.000	.054	6.000	.000	6.033	.000	6.087
AL	3.496	*	3.114	*	3.288	*	3.145	*	3.433	*	3.491	*	3.212	*	3.264	*
TI	.033	*	.025	*	.041	*	.062	*	.023	*	.042	*	.022	*	.052	*
CR	.001	*	.002	*	.005	*	.007	*	.001	*	.000	*	.000	*	.001	*
FE	.670	*	1.205	*	.952	*	1.155	*	.693	*	.721	*	1.239	*	1.175	*
MN	.163	*	.421	*	.262	*	.250	*	.116	*	.181	*	.459	*	.240	*
MG	.009	*	.014	*	.021	*	.012	*	.028	*	.018	*	.016	*	.019	*
CA	5.928	10.300	5.482	10.263	5.592	10.162	5.732	10.362	5.996	10.290	5.785	10.238	5.354	10.303	5.388	10.139
O	24.000	*	24.000	*	24.000	*	24.000	*	24.000	*	24.000	*	24.000	*	24.000	*
	GROS	87.56		76.97		81.91		80.18		87.76		86.28		75.74		78.98
	ANDR	9.90		16.92		13.94		16.16		10.14		10.75		17.53		17.23
	PYR	2.54		6.10		4.15		3.66		2.11		2.97		6.73		3.79
	F/M	90.135		115.304		58.137		119.553		29.323		48.938		103.834		75.908
	F/FM	.989		.991		.983		.992		.967		.980		.990		.987

1 *****GAL 5 - C4 - GAR - SPOT 1
2 GAL 5 - C4 - GAR - SPOT 2
3 GAL 5 - C4 - GAR - SPOT 3
4 GAL 5 - C4 - GAR - SPOT 4
5 GAL 5 - C4 - GAR - SPOT 5
6 GAL 5 - C4 - GAR - SPOT 6
7 GAL 5 - C4 - GAR - SPOT 7
8 GAL 5 - C4 - GAR - SPOT 8

Appendix C: XRF and ICP-AES Bulk Rock Geochemistry Results

ACCURASSAY LABORATORIES
1046 Gorham Street
Thunder Bay, ON
Canada P7B 5X5
Tel: (807) 626-1630
Fax: (807) 622-7571
www.accurassay.com
assay@accurassay.com

Tuesday, January 31, 2012

Certificate of Analysis

Roderick Tom-Ying
University of Western Ontario 12
London , On, CAN

Ph#: (519) 870-1168
Email: rtomying@uwo.ca

Date Received: 12/30/2011
Date Completed: 01/26/2012
Job #: 201145035
Reference:
Sample #: 12

Acc #		Client ID	Al203 %	Ca0 %	Cr203 %	Fe203 %	K20 %	Mg0 %	Mn0 %	Na20 %	P205 %	Si02 %	Ti02 %	L0I %	Total %
332196		GAL-4	11.874	6.940	0.020	17.837	0.500	3.299	0.230	2.390	0.149	48.797	1.410	6.250	99.697
332197		GAL-5	12.964	12.520	0.120	11.097	0.220	5.760	0.531	2.320	0.060	51.266	0.721	1.300	98.878
332198		GAL-6	15.124	3.409	0.080	2.959	1.190	1.030	0.040	4.990	0.080	69.641	0.300	0.800	99.644
332199		GAL-8	14.984	3.230	0.180	3.550	1.070	0.920	0.050	5.610	0.071	68.220	0.300	1.350	99.536
332200		GAL-9	13.444	0.890	0.060	1.019	3.179	0.230	0.030	4.771	0.030	76.341	0.070	<0.001	100.063
332201		GAL-10	15.764	3.650	0.091	3.200	1.430	1.260	0.040	5.000	0.071	67.180	0.300	1.450	99.436
332202		MIN 21-1	13.854	14.170	0.120	11.398	0.390	5.340	0.200	0.770	0.071	51.718	0.761	1.550	100.342
332203		MIN 21-2	13.534	9.270	0.140	15.436	1.070	8.040	0.210	1.820	0.080	47.246	0.921	2.000	99.768
332204		MIN 21-3	14.494	11.200	0.099	12.977	1.070	6.799	0.210	2.440	0.071	48.436	0.831	1.150	99.779
332205		MIN 21-4	16.365	5.010	0.151	5.298	1.539	1.370	0.080	5.840	0.199	61.730	0.500	1.450	99.532
332206	Dup	MIN 21-4	16.824	4.820	0.140	5.188	1.500	1.310	0.080	5.590	0.211	62.089	0.490	1.450	99.692
332207		MIN 21-5	13.814	9.890	0.110	12.347	0.170	6.130	0.240	2.310	0.071	53.117	0.831	0.550	99.579
332208		MIN 22-1	13.334	8.530	0.159	8.508	1.909	10.490	0.130	3.180	0.291	47.997	0.611	3.950	99.090

PROCEDURE CODES: ALP1, ALAR1, ALXR1

Certified By: Jason Moore, General Manager

Table 1: Results from XRF Geochemistry.

ACCURASSAY LABORATORIES
1046 Gorham Street
Thunder Bay, ON
Canada P7B 5X5
Tel: (807) 626-1630
Fax: (807) 622-7571
www.accurassay.com
assay@accurassay.com

Thursday, January 26, 2012

Certificate of Analysis

Roderick Tom-Ying
University of Western Ontario \\\\\\\' 12
London , On, CAN

Ph#: (519) 870-1168
Email: rtomying@uwo.ca

Date Received: 12/30/2011
Date Completed: 01/26/2012
Job #: 201145035
Reference:
Sample #: 12

Acc #	Client ID	Ag ppm	Al %	As ppm	B ppm	Ba ppm	Be ppm	Bi ppm	Ca %	Cd ppm	Co ppm	Cr ppm	Cu ppm	Fe %	K %	Li ppm	Mg %	Mn ppm	Mo ppm	Na %	Ni ppm	P ppm	Pb ppm	Sb ppm	Se ppm	Si %	Sn ppm	Sr ppm	Ti ppm	Tl ppm	V ppm	W ppm	Y ppm	Zn ppm
332196	GAL-4	<1	2.85	3	63	27	<2	15	2.47	4	35	110	395	7.09	0.27	25	1.22	968	9	0.36	<1	689	13	<5	<5	0.14	<10	37	3590	273	158	<10	17	102
332197	GAL-5	<1	1.57	<2	58	5	<2	17	2.58	<4	17	271	104	2.49	0.07	5	0.77	1120	<1	0.22	<1	293	6	<5	<5	0.10	<10	26	2413	161	71	<10	11	38
332198	GAL-6	<1	1.28	2	55	98	<2	5	0.79	<4	9	259	19	1.56	0.48	19	0.52	276	<1	0.16	<1	350	<1	<5	<5	0.06	<10	56	1476	285	28	<10	3	36
332199	GAL-8	<1	1.56	<2	63	154	<2	<1	1.23	<4	11	548	28	2.16	0.62	22	0.58	301	1	0.31	<1	288	2	<5	11	0.09	<10	84	1448	167	37	<10	3	47
332200	GAL-9	<1	0.37	2	56	65	<2	<1	0.48	<4	<1	192	3	0.30	0.26	4	0.02	153	3	0.11	<1	<100	15	<5	8	0.03	<10	34	<100	240	<2	<10	2	40
332201	GAL-10	3	1.28	24	51	71	<2	7	0.91	186	15	280	287	1.78	0.37	20	0.52	192	<1	0.16	2	167	118	<5	12	0.05	<10	126	1139	170	22	346	2	57
332202	MIN 21-1	<1	1.86	<2	41	10	<2	7	2.74	<4	14	206	13	1.85	0.09	5	0.46	376	<1	0.07	<1	273	4	<5	6	0.09	<10	48	2632	251	60	<10	9	25
332203	MIN 21-2	<1	3.55	<2	49	80	<2	33	3.09	<4	45	342	222	6.31	0.62	50	2.53	1011	<1	0.26	43	339	9	<5	<5	0.18	<10	44	3668	125	145	<10	10	88
332204	MIN 21-3	<1	2.76	<2	53	74	<2	6	2.90	<4	34	250	247	4.42	0.71	36	1.67	785	<1	0.24	29	222	8	<5	<5	0.12	<10	104	3193	111	121	<10	10	82
332205	MIN 21-4	<1	2.13	<2	64	165	<2	13	2.15	<4	17	453	36	3.02	0.93	38	0.86	518	<1	0.35	<1	981	9	<5	<5	0.15	<10	237	2493	226	63	<10	6	84
332206D	MIN 21-4	<1	2.01	<2	49	165	<2	4	1.99	<4	15	445	20	2.81	0.90	36	0.77	476	<1	0.34	<1	974	3	<5	<5	0.14	<10	231	2295	240	56	<10	6	81
332207	MIN 21-5	<1	1.64	2	50	21	<2	1	1.84	<4	18	215	95	2.66	0.13	9	0.97	586	<1	0.24	<1	371	3	<5	<5	0.11	<10	43	2065	194	72	<10	6	40
332208	MIN 22-1	<1	2.55	<2	55	275	<2	12	2.83	<4	31	295	59	3.17	0.92	44	2.52	532	<1	0.24	112	1159	5	<5	5	0.13	<10	165	1969	179	72	<10	6	41

PROCEDURE CODES: ALP1, ALAR1, ALXR1

Certified By: Jason Moore, General Manager

Table 2: Results from ICP-AES Geochemistry.